




Article

Outdoor Microclimate in Courtyard Buildings: Impact of Building Perimeter Configuration and Tree Density

Lia Marchi , Jacopo Gaspari  and Kristian Fabbri 

Department of Architecture, University of Bologna, 40136 Bologna, Italy; jacopo.gaspari@unibo.it (J.G.); kristian.fabbri@unibo.it (K.F.)

* Correspondence: lia.marchi3@unibo.it

Abstract: As the effects of climate change and urbanisation intensify, liveability and comfort in outdoor spaces decrease. Because of large spaces exposed to solar radiation and low crossing of airflows, courtyard buildings are extremely vulnerable in this regard. However, there are significant gaps in the literature on outdoor comfort in courtyards, especially regarding the effect of border configuration (including gap position and features), as well that of tree density. The study proposes a methodology—to be used during preliminary design—to compare the effect of alternative scenarios for courtyard buildings on outdoor microclimate, varying both the building perimeter configuration and courtyard vegetation layout. A matrix is set to combine the two variables and select relevant scenarios, which are then simulated in ENVI-met focusing on air temperature, wind speed and physiological equivalent temperature (PET). A case study in Bologna, Italy (humid subtropical climate) is presented as an example of the implementation. The resulting outdoor microclimate maps and frequency diagrams are compared and discussed. It emerges that both variables have a role in outdoor comfort: while gap configuration affects air temperature more (up to a difference of 1 °C), tree density impacts PET by up to 2 °C difference. The methodology can be replicated in several other contexts to support the optimisation of courtyard building design from the early stages.

Keywords: outdoor microclimate map; outdoor thermal comfort; ENVI-met; air temperature; wind speed; PET



Citation: Marchi, L.; Gaspari, J.; Fabbri, K. Outdoor Microclimate in Courtyard Buildings: Impact of Building Perimeter Configuration and Tree Density. *Buildings* **2023**, *13*, 2687. <https://doi.org/10.3390/buildings13112687>

Academic Editor: Bo Hong

Received: 5 October 2023

Revised: 20 October 2023

Accepted: 23 October 2023

Published: 25 October 2023



Copyright: © 2023 by the authors. Licensee MDPI, Basel, Switzerland. This article is an open access article distributed under the terms and conditions of the Creative Commons Attribution (CC BY) license (<https://creativecommons.org/licenses/by/4.0/>).

1. Introduction

Scientists from the Intergovernmental Panel for Climate Change (IPCC) predict a 1.5 °C increase in global temperature due to climate change (CC) effects by 2050 in the best scenario, which means global emission reduction targets are achieved in time thanks to nationally determined contributions (NDCs) [1]. Even in this case, in Europe, annual mean temperature is expected to rise at least 1.6 °C and maximum temperature of the warmest month 1.9 °C in 2050 compared to the three previous decades (1985–2014) [2]. Additionally, the number of hot days and the duration (+63%) and frequency (+18.9%) of heatwaves are presumed to increase in all future climate change scenarios for Europe. Should we fail in achieving the set targets, these effects would dramatically worsen: +83.7% heatwave frequency and +1.247% heatwave duration in 2050.

Dense urban environments will be especially impacted, as well as the liveability and well-being of citizens. In particular, rising mean temperatures will exacerbate heat stress in cities [3], where “the modified land surface affects the storage and radiative and turbulent transfers of heat and its partition into sensible and latent components [. . .]. The relative warmth of a city compared with surrounding rural areas, known as the urban heat island (UHI) effect, arises from these changes and may also be affected by changes in water runoff, pollution and aerosols” [4].

Beyond the expected rising temperature, many researchers agree that the lack of green areas in favour of large impervious surfaces that absorb more energy and cool more

slowly is one of the main reasons that heat stress is higher in cities [5,6], along with the fact that building elevations and density reduce wind speed (air flow) and prevent heat dispersion [7–9]. In addition, human activities such as heating/cooling buildings and driving cars warm the environment.

As a result, people's comfort in outdoor spaces is highly affected, and pollutants are more likely stagnating in the air [10]. This in turn exacerbates climate-related discomfort and disease, including cardiovascular and respiratory disorders, as well as heat-stroke, leading to increased mortality rates [11–13], not to mention this discouraging people to spend their (free) time in uncomfortable public or collective outdoor spaces [14].

Other side effects of rising temperatures include the need for more cooling in buildings during the summer to maintain comfortable indoor temperatures. Taking Europe as an example, a rise of 59% in cooling degree days is expected in 2050. This value must be elevated to 305% should annual mean temperature rise surpass 2 °C [2]. These effects are already visible in larger European cities, such as the centres of London and Paris, which regularly record night-time temperatures 4 °C higher than rural surroundings [15].

Therefore, how to protect urban areas from heat waves is one of the most significant issues that policymakers, urban planners and designers need to address as soon as possible [7].

1.1. How to Mitigate Urban Heat Stress

Several strategies and designs are documented in the literature to this end, and their effects are increasingly being tested with the appropriate assessment methods [16–19]. The current knowledge is that the most impactful factors are vegetation, surface material properties, morphology of buildings, and wind-air flows [20].

On the one hand, great attention has been paid to the impact of urban surfaces on outdoor comfort, especially focusing on heat-related features of pavement and façade materials. Using reflective, permeable pavements with high albedo and reflectivity is a promising strategy to mitigate UHI [21]. The same is valid for cool or evaporative pavements [22,23].

Similar proprieties are sought in façade design, where it is preferable to select high-emissivity materials to improve the outdoor microclimate [24]. Notably, Alonso et al. point out that façades' colour, emissivity, and solar reflectance not only affect outdoor thermal comfort but also the building energy demand [25]. Zinzi also proves that 'cool façades' have the potential to mitigate outdoor heat stress while reducing the building demand for summer cooling [26]. However, visual comfort of pedestrian should be carefully considered when using these materials, in order to select options that both reduce heat stress and visual discomfort [27].

Several studies and applied cases demonstrate that cool materials have a greater mitigation effect when used on both buildings and the ground at the same time, as they result in a significant reduction in air and surface temperature [25,28,29], but their full potential has yet to be realised.

On the other hand, nature-based solutions (NBSs) such as tree planting, green permeable surfaces (e.g., grass) or water-based elements are receiving considerable attention [30,31]. Based on the green evapotranspiration principle that air is cooled by replacing sensible heat with latent heat [32], adding vegetation is quite a diffuse and effective mitigation strategy all over the world [33,34]. Additionally, water basin and water design elements are spreading as a way to improve outdoor microclimate in cities [35,36], even if the increasing scarcity of water due to CC might hamper the success of this strategy. Blue and green solutions are usually favourably welcomed by citizens because of the additional benefits for people and nature, including psychological relief [37]. However, their effectiveness depends on climate and context features, given that also building shadows and wind canyons can affect NBS functioning.

Urban geometry also influences the functioning of heat mitigation strategies [38], which explains why the morphology of blocks and buildings has been increasingly studied with relation to heat stress and especially ventilation effects.

1.2. Heat Stress in Dense Urban Patterns

Given that urban morphology—defined as “mass, density, and orientation of building stocks” [39]—strongly impacts natural ventilation, computational fluid dynamic simulations have been widely and increasingly used to investigate its effect on outdoor thermal comfort. In order to fully consider the many variables involved, assessment methods have evolved in the years from bidimensional indicators (e.g., building density or floor-to-area ratio) to three-dimensional ones (e.g., building volume, height, shape) [40–42].

In particular, dense urban environments have been proven to considerably worsen ventilation flows and thus affect thermal comfort at pedestrian level [43]. Therefore, Palusci and Cecere recommend urban renewal plans considering how airflows and urban morphology interact because their effects on human life can be either positive or negative [44]. However, most studies focus on idealised urban patterns [45], while studies of real neighbourhood or block layouts are still limited.

Building blocks or street grids do indeed shape urban structures, defining diverse densities and favouring or hindering dominant wind accordingly. In this regard, it has been noted that the historical city pattern, albeit dense and made of low-reflection materials, has irregular street geometries that benefit building mutual shading and thus preventing surfaces from being exposed to solar radiation for long periods of time. In this model, vegetation was typically concentrated in private or collective gardens.

Modern city concepts, with progressive enlargement of street sections and public spaces, may have aided wind flows if dominant directions were considered during the planning stage, but at the expense of the mutual shading effect. Because voids prevail on built elements, stones and construction materials are directly more exposed to solar radiation and thus embed more heat, exacerbating the heat island effect typical of cities. This is in fact proven by Oke, who demonstrates how historic European city patterns are more favourable in terms of climate than modern city forms, exemplified by North American ones [46]. Nowadays, it is largely acknowledged that cities with an orderly pattern, such as the street grid, have a much greater urban heat island effect than cities with a more disordered pattern [47].

This suggests that the diffused modern courtyard building type is among the most critical ones, with regular borders, large street section and unshaded spaces, which is why a significant body of literature exists to evaluate thermal comfort in courtyards [48–52].

1.3. Assessment of Outdoor Comfort in Courtyards

As the attention towards thermal comfort in courtyards has grown, methods and tools for evaluating it have also advanced, whether through on-site monitoring, computer simulations, or a combination of both [51]. Also, design-support procedures to optimise courtyard inner space layout for building microclimate have been developed [53]. In most cases, simulations of outdoor thermal comfort in courtyards are based on ENVI-met software [54–57], which returns maps on air, soil and building surfaces, as well as the thermal comfort expressed through the Physiological Equivalent Temperature Index (PET), the Universal Thermal Climatic Index (UTCI) and the predicted mean vote (PMV) [58]. PET, in particular, is defined by Höppe [58] as “the air temperature at which, in a typical indoor setting (without wind and solar radiation), the heat budget of the human body is balanced with the same core and skin temperature as under the complex outdoor conditions to be assessed”. Therefore, the software allows consideration of all relevant parameters that affect outdoor thermal comfort in a three-dimensional microclimate model, from vegetation to building morphology and surface materials.

Many scholars examined the shading effect carried by the shape, orientation, and boundary surfaces (such as building walls) of courtyards in order to enhance open space

comfort [49,50,52,59,60]. Several authors addressed the benefits of vegetation and cool pavements within courts [61,62]. Taleghani et al., as an example, argue that in courtyard blocks in the Netherlands, the use of greenery on both roofs and pavements is the most effective strategy to mitigate heat stress [63]. The effect of tree planting on courtyard outdoor comfort is also particularly studied [64–66].

Fewer studies focus on airflows in courtyards to reduce heat stress, either indoor or outdoor [67–70]. The same limited attention is paid to the effect that the volume distribution on the borders may generate on courtyard outdoor thermal comfort, that is, the effect of building elevation features and the positioning of floor-to-ceiling gaps or access breaches. This might instead be of great help both in cases of new developments or urban regeneration plans to predict the effect of design choices on outdoor thermal comfort.

A recurring approach in contemporary developments is to symmetrically locate the volumes on the borders of the plot according to regular patterns providing access to the inner courtyard through breaches that interrupt the elevation continuity on each side of the plot, mainly to give a semi-public character to this space. Less frequently, these gaps follow an irregular distribution that is mainly due to the relation with surrounding alignment, passages, or street directions. Not only does the different distribution and nature of these volumes influence the way the courtyard space can be naturally ventilated but also the distribution of vegetation (if any).

The investigation of this topic can be highly relevant to provide solutions in existing contexts, where new volumes are built in the gaps between existing buildings to contrast urban sprawl by exploiting available voids. The practice of inserting new buildings along existing discontinuous urban fronts is taking pace, encouraged by several municipalities worldwide, and many guidelines have been published accordingly, but at present no one has mentioned the potential impact of such interventions on the courtyard thermal comfort [71–74].

Accordingly, it is worth investigating how building continuity or discontinuity, gaps, and the nature of possible vegetation patterns can affect the outdoor microclimate of courtyards, which represents an interesting, recurring, and still critical typology for many reasons.

2. Goals

The aim of this study is thus to investigate the role of courtyard building perimeters and courtyard vegetation in affecting the microclimate to improve outdoor thermal comfort in open spaces. In particular, the specific objective is to explore the impact of two elements that are recurrently considered in courtyard building design: (i) volume distribution along the courtyard borders, and how the gaps are treated to screen ventilation air flows or not; and (ii) vegetation distribution in the courtyard.

3. Materials and Methods

The methodology compares the effect of alternative scenarios for courtyard buildings on outdoor microclimate, varying both the building perimeter configuration and courtyard vegetation layout. The procedure is relevant to new buildings design as well as redevelopment projects to foresee and thus optimize courtyard thermal comfort.

Outdoor microclimate maps (OMMs) are used to investigate their effects assuming air temperature, wind speed and PET as the most significant indicators [75,76]. To this end, the study makes use of the ENVI-met software (v 5.5), as the most used and reliable to simulate ventilation in urban environments, especially when it is necessary to consider the interaction of different surface materials, vegetation, and solar radiation with air flow and its turbulent phenomena [67]. Accuracy level and calibration of the tool are also reported in [77]. This study aims to simulate the effect of two main design variables, focusing on:

- (A) The building perimeter configuration, including both gap positioning and their capacity to influence airflows.

In fact, the border features may vary depending on the skyline, urban morphology and density, front alignments, and functional requirement, so different options are explored, from simple breaches between volumes, to continuous fronts where the gaps are filled with volumes, passing through intermediate solutions where screens are placed in the gaps to ‘modulate’ airflow crossing.

(B) Vegetation distribution, especially focusing on tree density.

The courtyard layout as well can vary according to contextual factors and diverse uses (e.g., public or collective spaces, parking areas, etc.). In particular, among the possible NBSs to be implemented, the study focuses on tree planting as the most frequent in courtyard buildings.

As a first step in the design process that is here simulated, all possible gaps are positioned in the courtyard perimeter according to the plot and building size. Then, several scenarios corresponding to alternative perimeter configuration can be defined, by respecting local planning rules and context constraints (e.g., minimum distance from windows of other buildings) while ensuring adequate access to the courtyard. This may lead to some gaps to be maintained mandatorily open (i.e., void).

The basic principle behind defining scenarios is to simulate the impact of the two variables on a gradient basis, as shown in Figure 1:

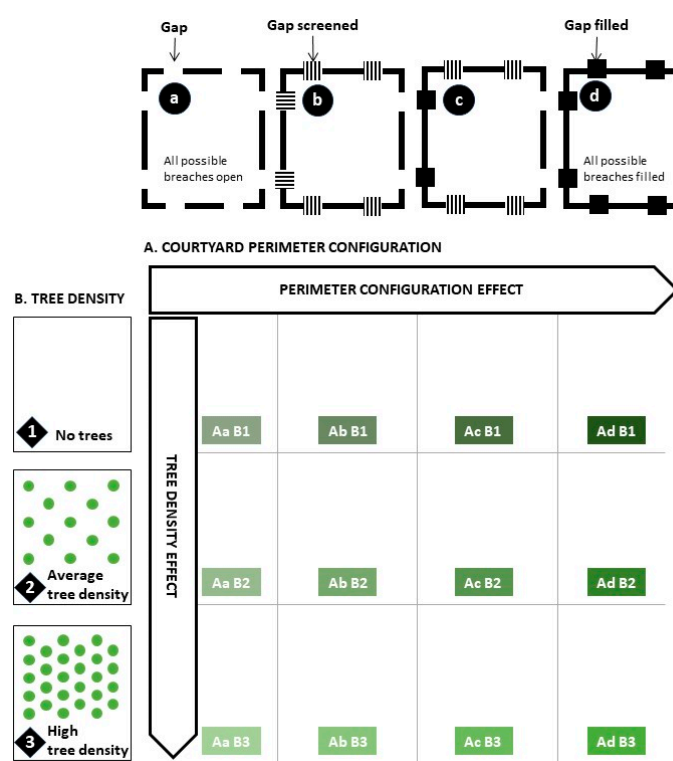


Figure 1. Concept map to select scenarios to be investigated. Perimeter features are indicated by letters, tree density by numbers.

- (A) from a courtyard building with multiple accesses (Aa—all possible gaps are left open) to a continuous courtyard building (Ad—all gaps filled), passing through intermediate situations in which some gaps are only ‘screened’ to align the frontages and others are filled with proper volumes;
- (B) from no trees (B1) to a high tree density (50–70% of the courtyard surface) (B3).

In the case of an existing building, all scenarios must be compared with the actual case study situation (scenario 0) to ensure current conditions are not worsened. Once the scenarios to be analysed are selected, the effects of variables A and B are simulated through

OMMs by the ENVI-met software (v 5.5), especially considering air temperature (measured in °C), wind speed (m/s) and physiological equivalent temperature (PET, °C).

A significant day of summer where peak heat stress is expected must be assumed in the setting for the simulation, which is run for a 48 h time span assuming the hottest day as a reference and the previous one as a double check. Then, results from three representative hours of the day with regard to heat stress are compared: e.g., 11:00 for the morning (when the temperature starts to significantly rise), and 13:00 (maximum solar radiation) and 15:00 for the afternoon (when the effects of the peak heavily affect the microclimate).

PET is calculated assuming conventional parameters of metabolism, clothing and activity for an adult person. Accordingly, assuming the range scale proposed by Matzarakis et al. [78], the output is reported on a six-factor scale: below 23 °C corresponds to thermal sensation 'slightly warm', 23 °C–29 °C 'warm', 29 °C–35 °C 'hot', 35 °C–41 °C 'very hot', 41 °C–47 °C 'extremely hot', and above 47 °C 'extreme heat stress/collapse'.

The process (Figure 2) is considered validated by comparing the simulated scenario 0 with onsite measurements for calibration purposes. This has been already investigated by the authors in previous studies where ENVI-met results' consistency and reliability with real data were demonstrated with reference to the calibration of outdoor microclimate simulation models [77].

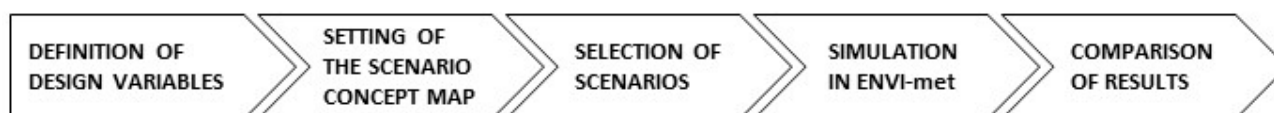


Figure 2. Concept of the methodological steps.

To this end, it is worth clarifying that the goal of the study is not focusing on refining data accuracy, but to exploit a consolidated approach to investigating the impact of courtyard perimeter configuration and tree density variations through OMMs. The adoption of a digital environment for this simulation is particularly helpful, especially when alternative scenarios—which cannot all be realised—must be compared.

4. Case Study

A case study is used only to clarify the methodology and not to compare the accuracy of the simulation outputs with real data. Any other intervention on courtyard buildings in a different place have been potentially selected. In this case, an infill development within a social housing courtyard building was chosen as representative of a regeneration process that many Italian and European cities are undergoing.

The site is located in the city of Bologna (Italy), 44° 49' N latitude, 11° 34' E longitude and 50 m a.s.l. altitude. According to the Köppen–Geiger classification [79], the area falls within a humid subtropical climate (Cfa) with short dry summers and heavy precipitation during mild winters. The city is in the Italian climatic 'zone E', where the number of degree days (DDs) is estimated between 2101 and 3000.

The building is located in Bolognina, a district north of the railway station that has the highest rate of social housing in the city due to its historic position as a working-class neighbourhood. In this city, the municipality and ACER Bologna (local public housing agency) have begun a broad and ambitious programme to renovate the stock while dealing with climate change and social issues.

The original urban plan was based on a regular grid of streets defining plots with courtyards, which have been partly reshaped during the post-war reconstruction. An infill development is planned in a specific courtyard (Figure 3) that is fully devoted to social housing and whose central open space is now used as a parking area by the residents, with negative consequences in both its usability and liveability.

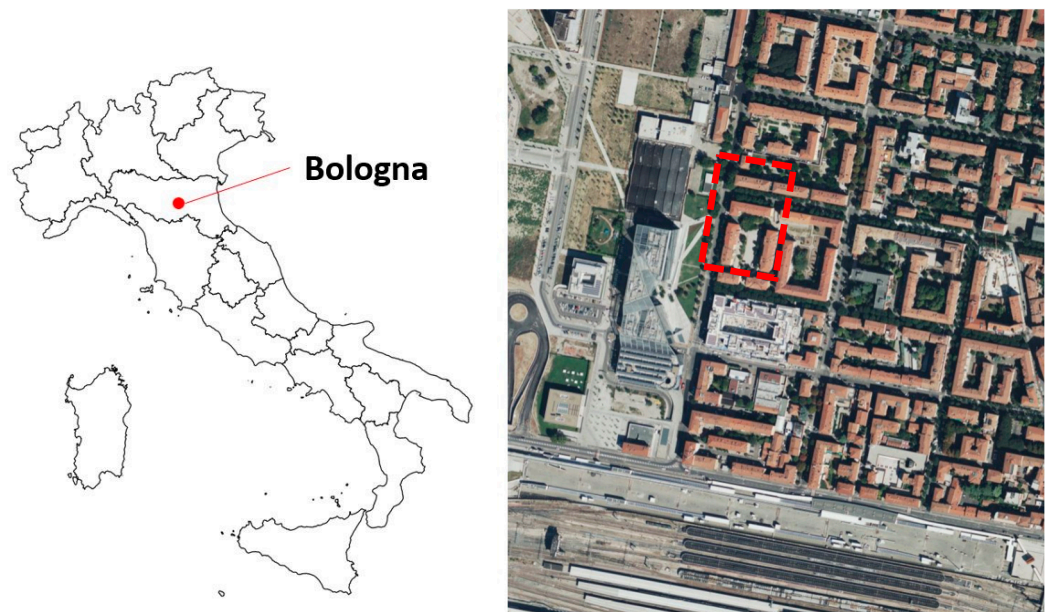


Figure 3. The city of Bologna (left) and aerial view of the area, with case study highlighted in red. Source: Bing maps.

The inner courtyard is 35×70 m (2100 m²), with 18 m-tall buildings on the border. The current breaches in the block's perimeter measure 8 m in width. The project (Figure 4) brief is to redesign the courtyard landscape features to improve outdoor thermal comfort and lessen local heat stress while clearing central areas from cars, reconfiguring urban fronts, and including some new dwellings to cope with the chronic shortage of housing. Once mandatory accesses are fixed, all other possible gaps to work with are identified. Two design options are considered:

- (1) gaps filled with new buildings hosting additional dwellings, which do not allow airflow crossing;
- (2) gaps screened with automated parking volumes whose façades in perforated metal grids partially allow airflow crossing.

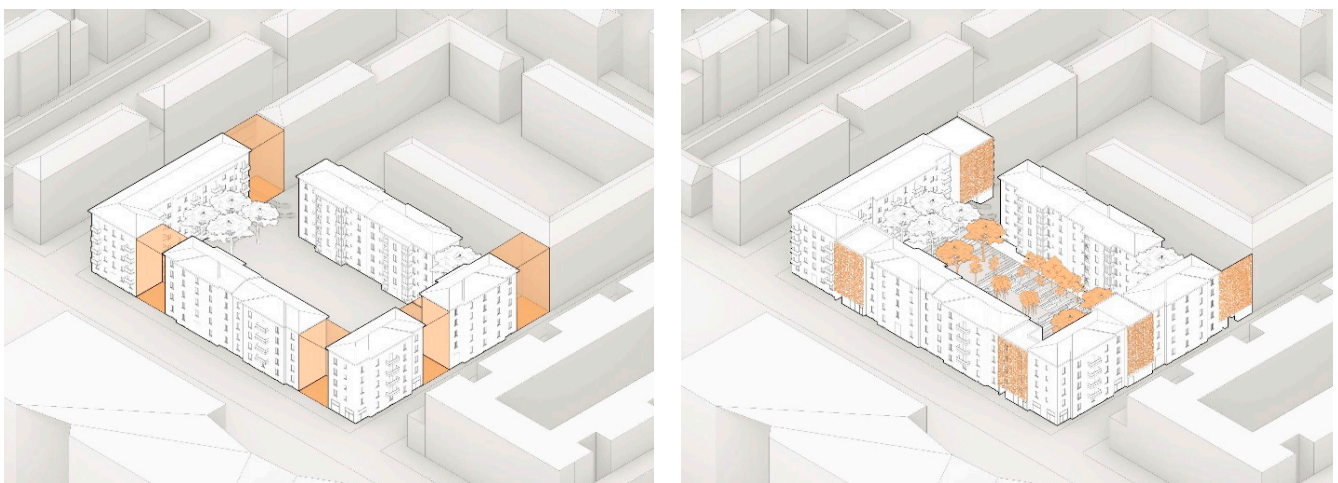


Figure 4. The sketch illustrates current gaps of the courtyard border that may be potentially filled (on the left) and a design proposal for the courtyard layout (on the right). Elaborated by I. Beijtaga.

The courtyard greening design is influenced by the decision of the public administration to favour the use of trees in semi-private open spaces as a mitigation strategy to

ensure their liveability as gathering places for the local community. Accordingly, only the tree pattern influencing the vegetation density was considered for the simulation.

From all the combinations possible, five have been selected for the simulation against the actual state (scenario 0). As the case study is analysed for demonstration purposes, some theoretical assumptions corresponding to extreme scenarios have also been included in the process in addition to the ones meeting optimal combinations from the concept map. This is aimed at better understanding the specific contribution of each variable.

Therefore, results have been compared in two main steps: one focusing on the effects of changes in the A variable, the second due to changes in B.

Figure 5 shows the selected scenarios, where Aa-d maintain the same tree density (i.e., average B2) but it changes the building perimeter configuration:

- Current state of the building block with existing gaps (scenarios Aa B2)
- All possible gaps are screened (scenario Ab B2)
- Some gaps are screened, and others are filled with new volumes (scenario Ac B2)
- All gaps are filled with new volumes (scenario Ad B2)

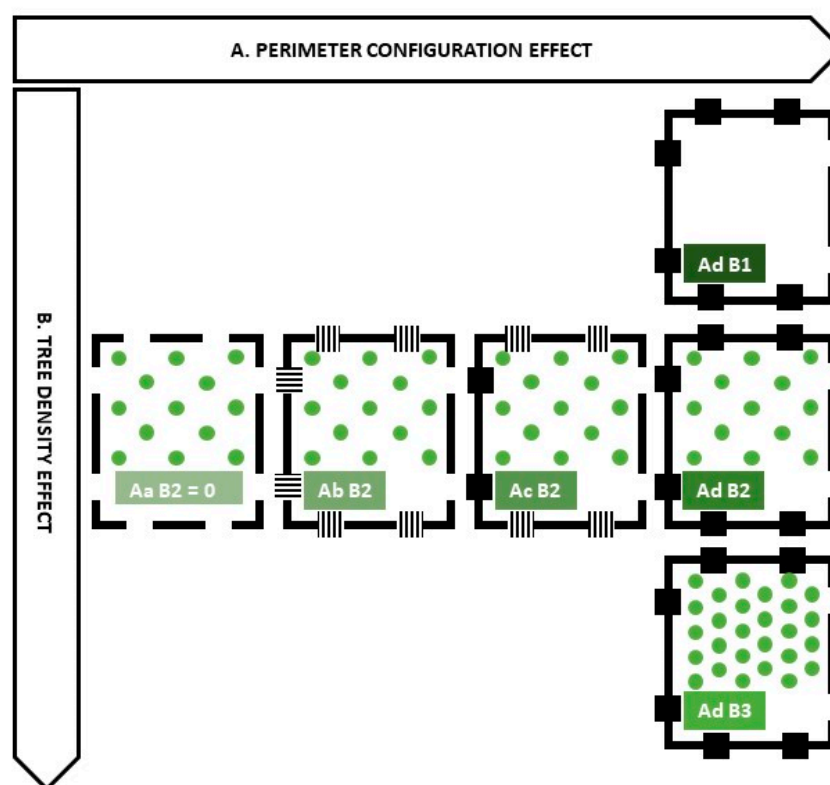


Figure 5. Concept map with selected scenarios.

Two gaps are left open in all the cases, as they are mandatory access for the courtyard. With reference to tree density, three conditions with all possible gaps filled (Ad) are simulated beside the current state (in this case, scenario 0 corresponds to Aa B2), which is taken as a means of comparison. Scenarios Ad B1–3 in fact consider the building perimeter as totally closed to evaluate the contribution of vegetation alone:

- no trees (0 tree), scenario Ad B1;
- average tree density (approximately 30% of the surface covered by trees), scenario Ad B2;
- high tree density (approximately 60% of the surface covered by trees), scenario Ad B3.

Trees are positioned in the ENVI-met model according to diverse possible functions of each courtyard portion. The pavement is considered impervious in all scenarios as it is in the current condition, and changing this surface would further influence the impacts by introducing a third variable that is not under investigation at this stage.

ENVI-met simulation was run for 12 August 2021, the hottest day of that year from the historic data set. Input climate data are from the local environmental database *Dext3r* from ARPAER [80,81]. For more reliable results, the simulation started from 6:00 the day before (11 August) and lasted 48 h. As for human parameters, the following choices were applied: a man 1.75 m height, 75 kg weight, 0.5 clo and slightly walking.

5. Results and Discussion

Results of the ENVI-met simulations are presented and commented on using both OMMs and frequency diagrams. The maps illustrate the spatial distribution of the values for each considered variable (air temperature, wind speed, PET) in the three selected hours. The diagram instead shows the value of these variables on the x -axis (one at a time) and their frequency in the OMM on the y -axis, i.e., the ratio of cells registering this value in the maps.

5.1. Outdoor Microclimate Maps, Variable (A) Perimeter Configuration Effect with Average Tree Density

The first set of OMMs show how volume positioning and the diverse combinations of filled and screened gaps affect outdoor thermal comfort. Regarding the air temperature at 11:00 (Figure 6, first column), values in the courtyard are between 31.5 °C (dark blue) and 32 °C (light blue), almost evenly distributed in scenarios Ab B2 and Ac B2, while in the current state (scenario Aa B2), there are areas with temperatures slightly higher: 32.5 °C and 33 °C (green).

At 13:00 (Figure 6, second column) the same homogeneous temperature distribution occurs, but one degree higher (32.5 °C and 33.5 °C), except for scenario Ad B2, where the temperature of the whole yard is 32.5 °C (green). Scenario Aa shows a greater variation in the air temperature of the courtyard, with values between 33 °C and 34 °C (red). At 15:00 (Figure 6, third column), the distribution is similar to that of 13:00, both in terms of distribution and values, except for the current state, which shows temperature lower by 0.5 °C.

From the comparison between the current state (Aa—multiple gaps in the courtyard building border) and progressive filling of the border, it emerges that gap screening can reduce courtyard air temperature by at least 1 °C. When all the possible gaps are filled with buildings, the courtyard air temperature is further reduced by 1 °C.

Figure 7 shows the frequency of each thermal comfort variable value in scenarios for the design variable A. The air temperature graphs show that at 11:00, the range is mostly between 30.5 °C and 32.5 °C, while at 13:00 and 15:00, the range is between 32 °C and 34.5 °C. In all graphs, the current scenario (Aa B2, blue line) shows the highest frequency of highest temperature values: at 11:00 45% of the area is at 32 °C, at 13:00 48% is at 33.5 °C and at 15:00 over 50% of the area is at 33.5 °C. The other scenarios have lower values, both in terms of peaks and of the range of the distribution: in fact, the frequency of the values is evenly distributed, except for scenario Ab B2, which has a higher frequency (peak) of lower values by approximately 1 °C compared to the others: at 11:00, 35% of the area is at 31 °C, at 13:00, 42% is at 32.5 °C and at 15:00, at least 50% of the area is at 32.5 °C. The other two scenarios have similar and homogeneous distribution. Surprisingly, the 'all possible gaps filled' scenario (Ad B2) is not the one with the largest area with lower temperature values.

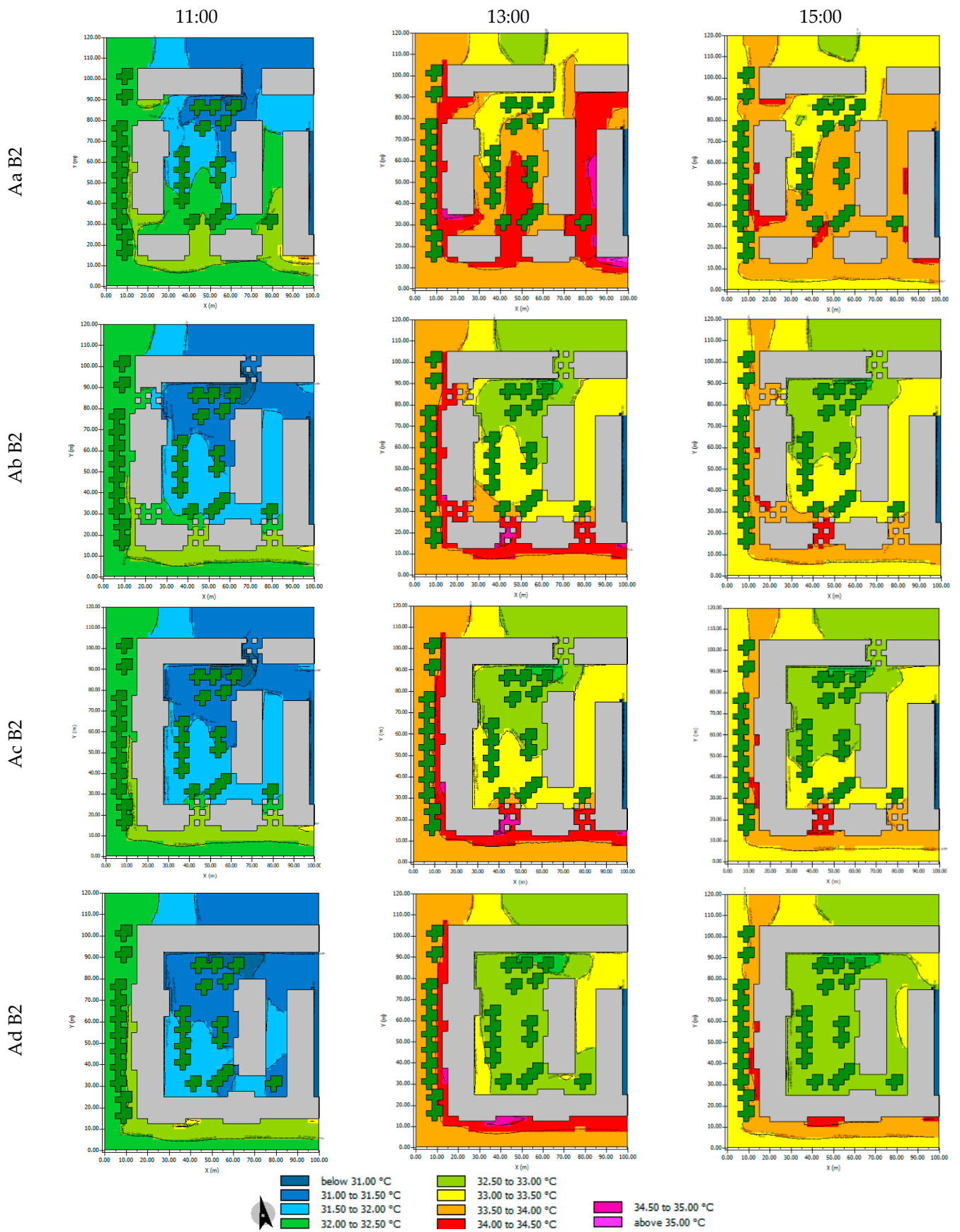
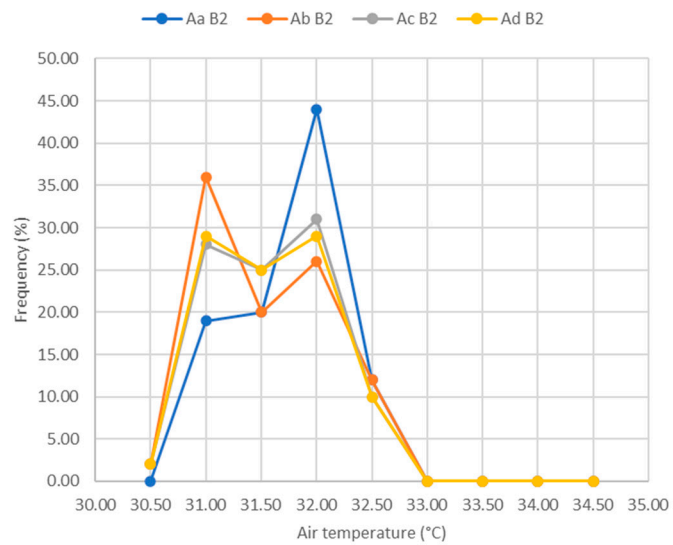
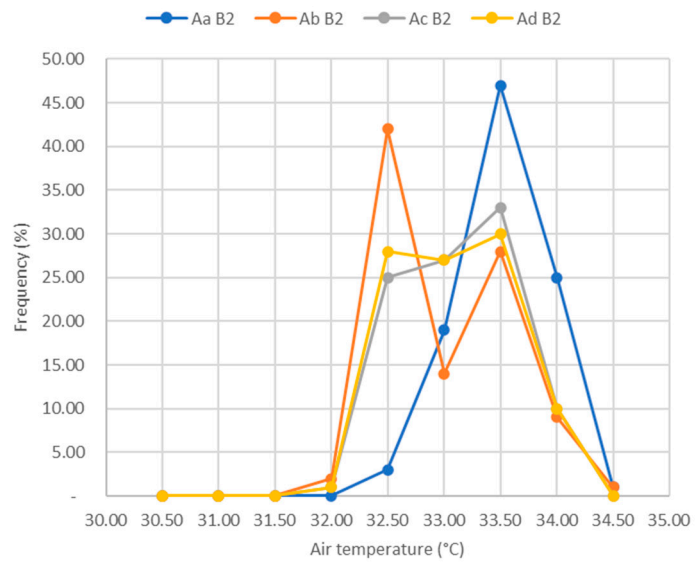


Figure 6. OMM showing the effects of variable A (block’s perimeter features) with average tree density—air temperature.

11:00



13:00



15:00

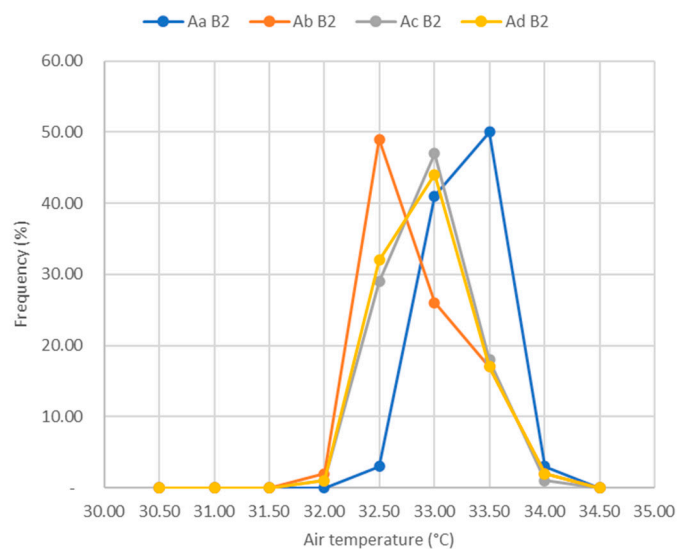


Figure 7. Variable A: OMM frequency of each variable, per selected hours and scenarios—air temperature.

Regarding wind speed (Figure 8), it should be considered that Bologna is in the Pianura Padana area, which has weak ventilation and no wind, just breeze less than 3–4 m/s. Hence, wind speed is typically about 0 m/s (calm, no wind) and always below 1.5 m/s (light air according to Beaufort scale). In the case study, higher speeds could be due to the Venturi effect near the gaps. Indeed, in the current case, at 11:00, wind speed between 3 m/s and 4 m/s is registered near the breaches. In the other scenarios, the air speed inside the courtyard is calm (0 m/s, blue) or light (0.5 m/s–1.5 m/s, blue), with slightly higher values (2 m/s, green) outside the courtyard. No significant variations are predicted by ENVI-met for 13:00 or 15:00. The ventilation of the courtyard is basically due to the Venturi effect near the gaps. Otherwise, the typical condition is calm or light air.

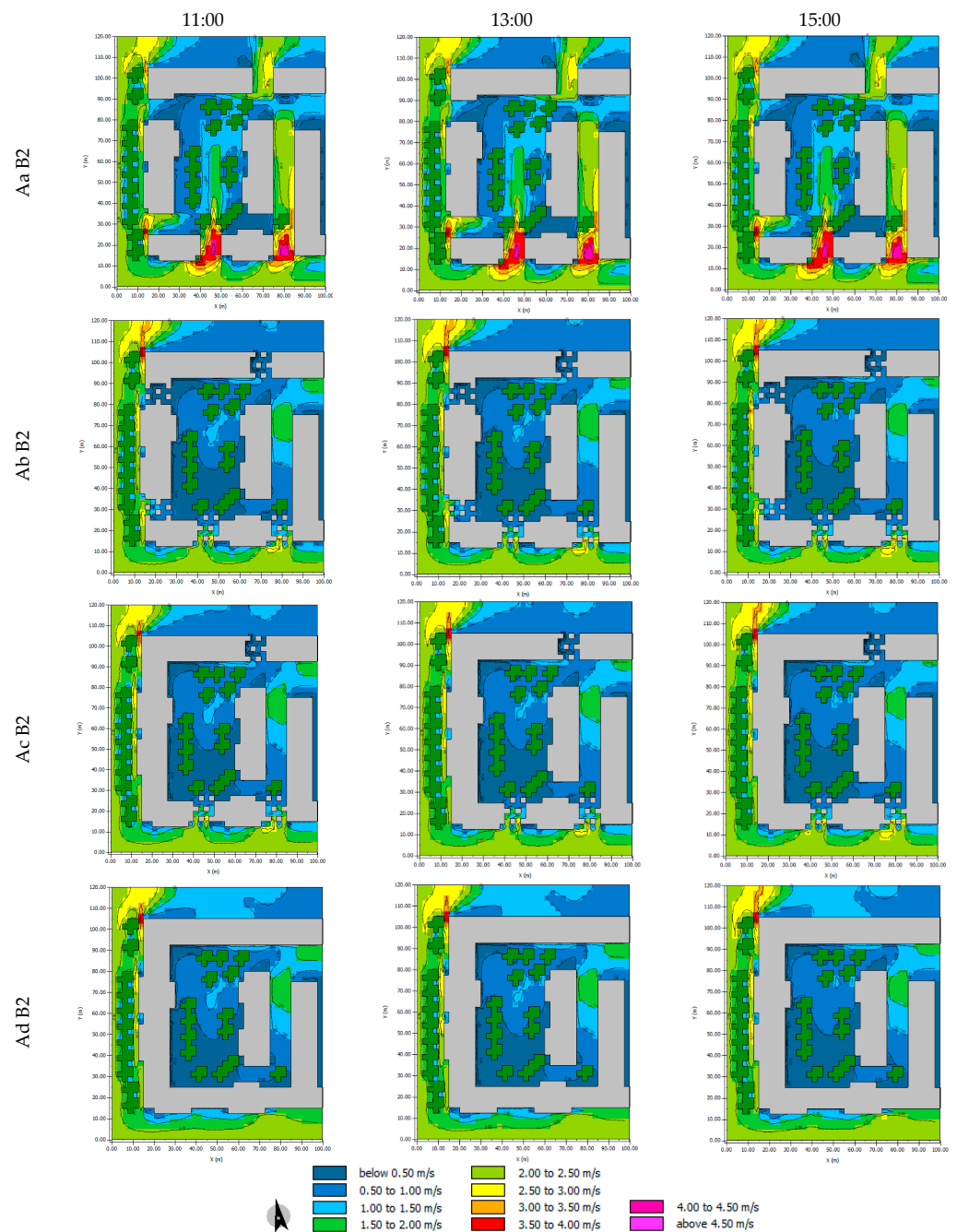
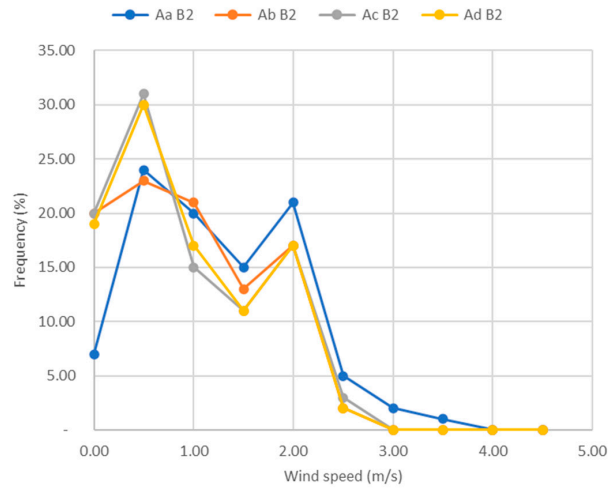


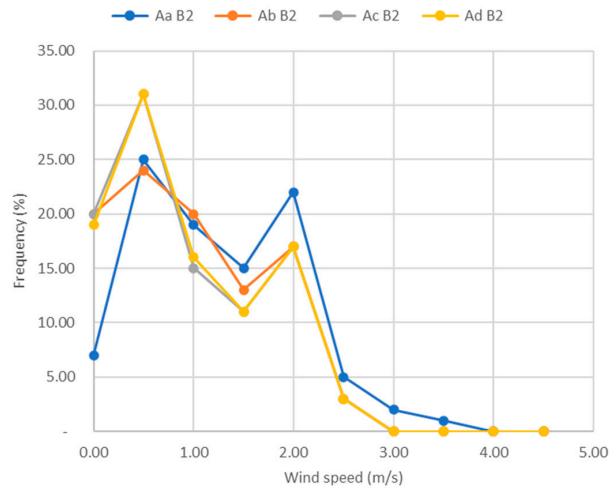
Figure 8. OMM showing the effects of variable A (block’s perimeter features) with average tree density—wind speed.

Figure 9 confirms that most of the area has wind speed values lower than 2 m/s. The only remarkable difference is the comparison between the actual state scenario (Aa B2, blue line) and the fully closed courtyard (Ad B2, orange line), while in the actual state, there are points with an air speed higher than 3 m/s, and in the latter, they are—not surprisingly—completely absent, and the maximum peak is 2.5 m/s.

11:00



13:00



15:00

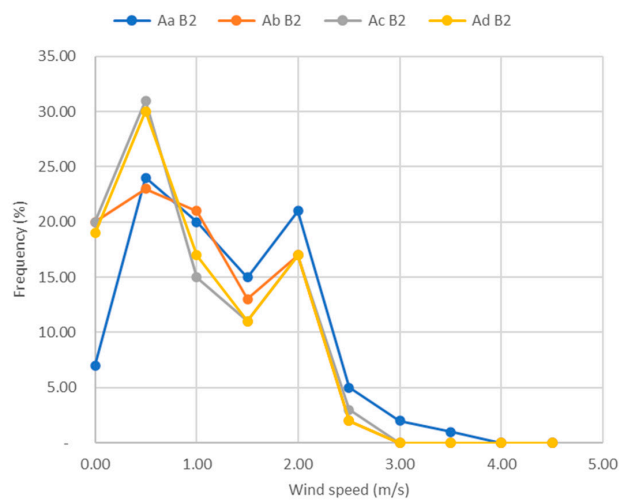


Figure 9. Variable A: OMM frequency of each variable, per selected hours and scenarios—wind speed.

PET (Figure 10) allows the simultaneous evaluation of multiple phenomena related to outdoor thermal comfort—such as air temperature, solar radiation, relative humidity and wind speed—with a single indicator.

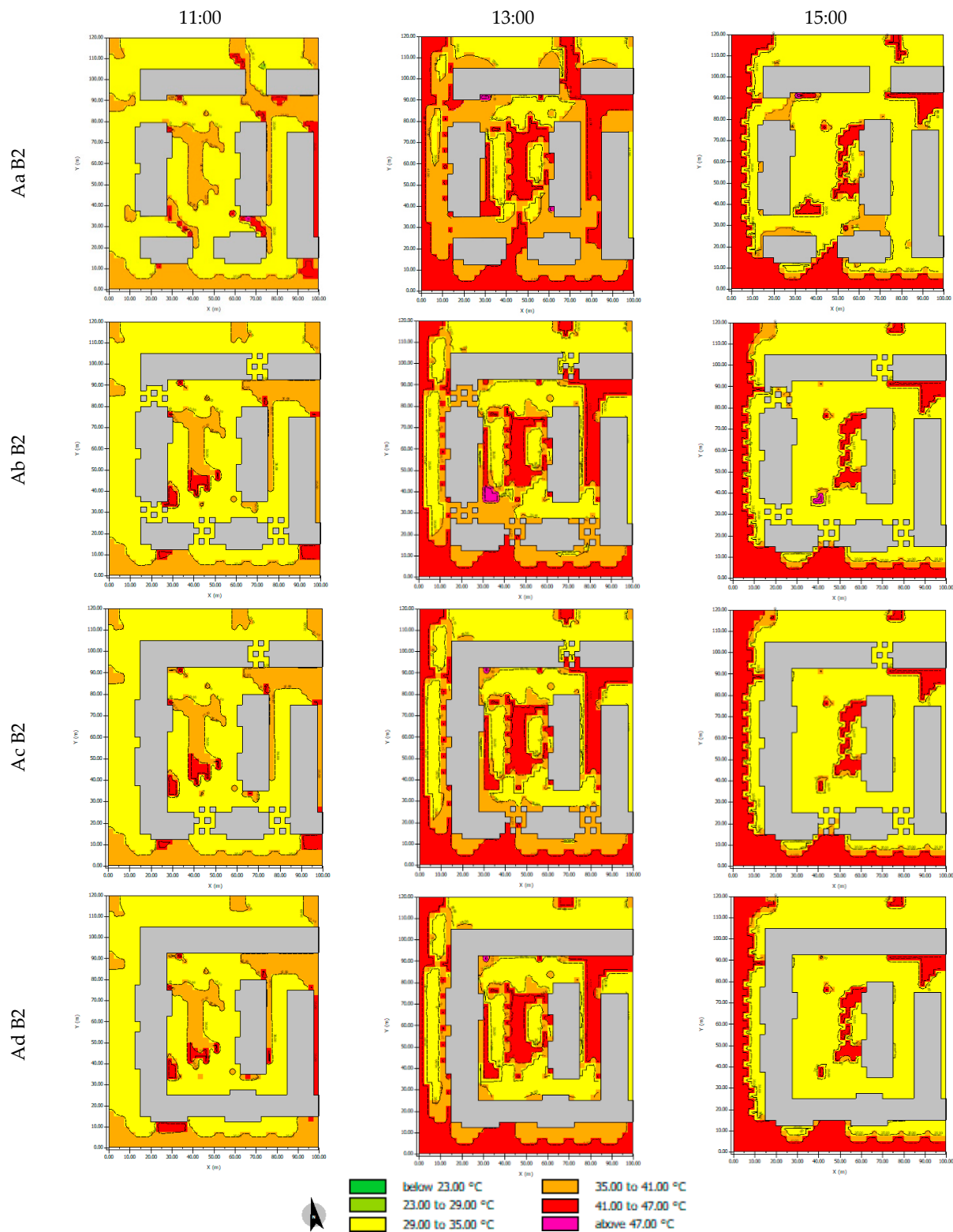


Figure 10. OMM showing the effects of variable A (block’s perimeter features) with average tree density—PET.

At 11:00, PET is nearly homogeneous inside the courtyard, as 29 °C–35 °C correspond to thermal sensation ‘hot’ (yellow), except for a central area with ‘very hot’ (35 °C–41 °C, orange) and a peak ‘extreme hot’ (red), that depends on how the building’s shadows are projected on the courtyard surface.

At 13:00, the thermal comfort depends mainly on the building shadows projected on the courtyard pavement: in fact, at the courtyard centre with maximum solar radiation, the software returns an ‘extremely hot’ sensation (41 °C–47 °C, red). At 15:00, the same thermal comfort of the morning is illustrated, but in this case, results show only two values: 29–35 °C corresponding to thermal sensation ‘hot’ (yellow), and a central area with ‘extreme hot’.

PET graphs (Figure 11) show a significant difference between the actual state (orange line) and the ‘all gaps filled’ scenario (blue line), as the first has a higher frequency of ‘hot’ PET values (29 °C–35 °C) at all three times. Another interesting aspect concerns the frequency of the ‘extremely hot’ condition that does not emerge from the OMMs: at 13:00 and 15:00, it appears that 30% of Ad B2 has ‘extremely hot’ values (in the centre of the area), while the other scenarios all have values around 20%. Thus, it seems that the gaps play a role in influencing the PET by eliminating the most extreme conditions.

5.2. Outdoor Microclimate Maps, Variable (B): Tree Density Effect

The second set of OMMs shows the effect of tree density. The maps also include the current situation for comparison. Regarding the air temperature at 11:00 (Figure 12), in the scenario without trees (B1), the air temperature is 31.5 °C (light blue), while in the high-tree-density one (B3), the whole area is 31 °C or lower.

At 13:00, the air temperature in the treeless area (B1) is homogeneous and equal to 33 °C (yellow), while in the high-tree-density version, the values are 31.5 °C–32 °C (green): this difference increases at 15:00, when in the B1 scenario the air temperature rises to 33.5 °C (orange). Thus, it emerges that with the same configuration of the courtyard (all gaps closed), the greater presence of trees allows a reduction in temperature of 0.5 °C to 2 °C, depending on the time of day. Compared to the current situation, a reduction of 2 °C is evenly registered. However, the more trees, the less the airflow, due to Venturi effect in the courtyard.

Figure 13 shows the comparison of the frequency graphs for variable B. The air temperature shows that the no-trees version (Ad B1, orange line) has the maximum frequency of highest temperature values at all the three times comparable to the actual state. At 11:00, 52% of the area is at 31.5 °C, at 13:00, 48% is at 33.5 °C and at 15:00, 50% of the area is at 33.5 °C. Therefore, it can be observed that the ‘all gaps closed’ scenario has wider projected shadows, but without trees, it has temperature values similar or higher to the current state.

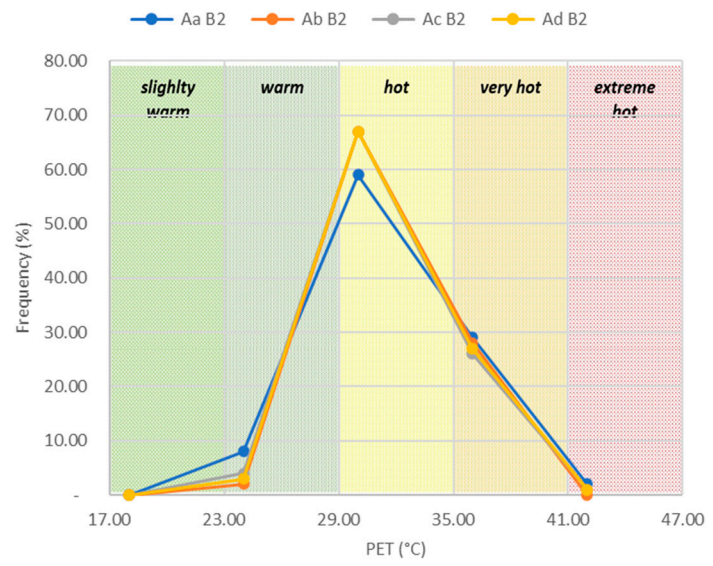
Figure 14 shows almost identical values of wind speed at the three times, particularly in the high-tree-density scenario where the air is calm. A Venturi effect can be seen in the no-trees scenario with a slight airflow near the openings on the left towards the courtyard on the right of the plot, but given the difference of only 0.5 m/s, this can be neglected.

The tree density effect is more significant in PET. At 11:00, the treeless scenario (B1) displays almost the whole area, with PET values equal to ‘extremely hot’ (red, 41 °C–47 °C), while in the high-tree-density scenario (B.3), PET is equal to ‘hot’ (yellow, 29 °C–35 °C) with a spike of two heat stress classes.

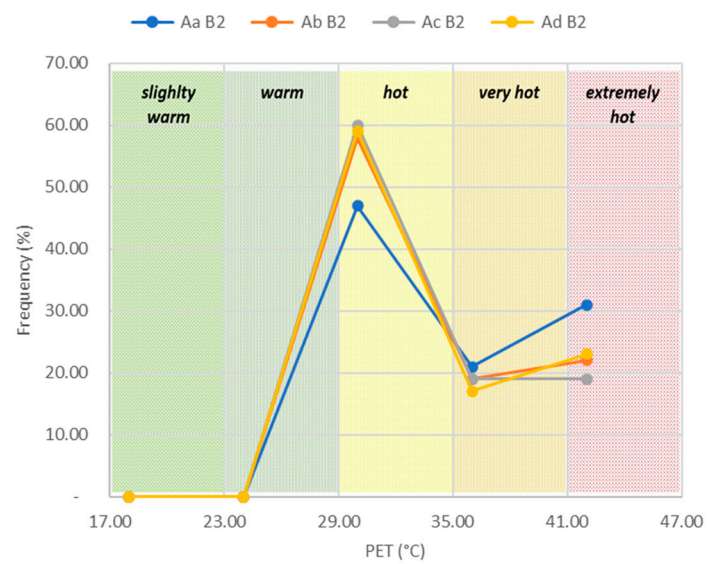
The same difference can be observed at 13:00 and 15:00, where there are also ‘collapse’ conditions (above 47 °C) in the no-trees situation. It is therefore evident that trees, thanks to the evo-transpiration principle, play a crucial role in influencing the outdoor heat stress, up to a leap of two heat stress classes.

The wind speed diagram (Figure 15) confirms what was said in the previous scenarios with variable A: the air is calm and below 2 m/s. In figures, the variations are not significant and are due to the values outside the courtyard building.

11:00



13:00



15:00

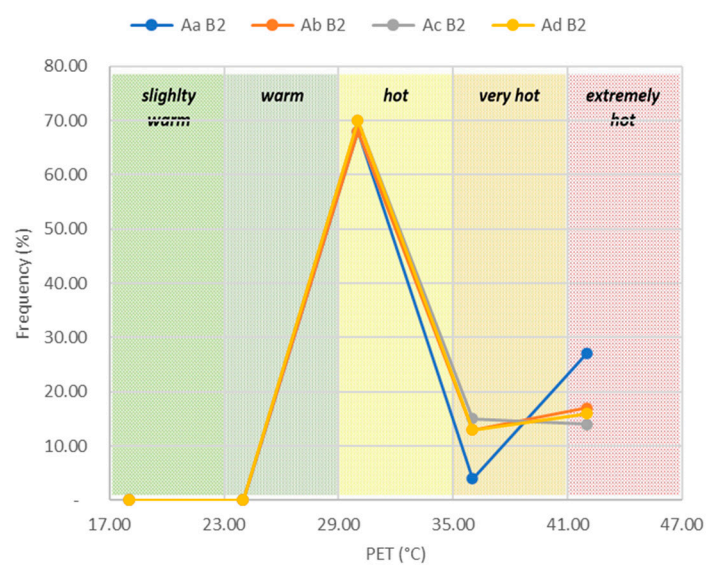


Figure 11. Variable A: OMM frequency of each variable, per selected hours and scenarios—PET.

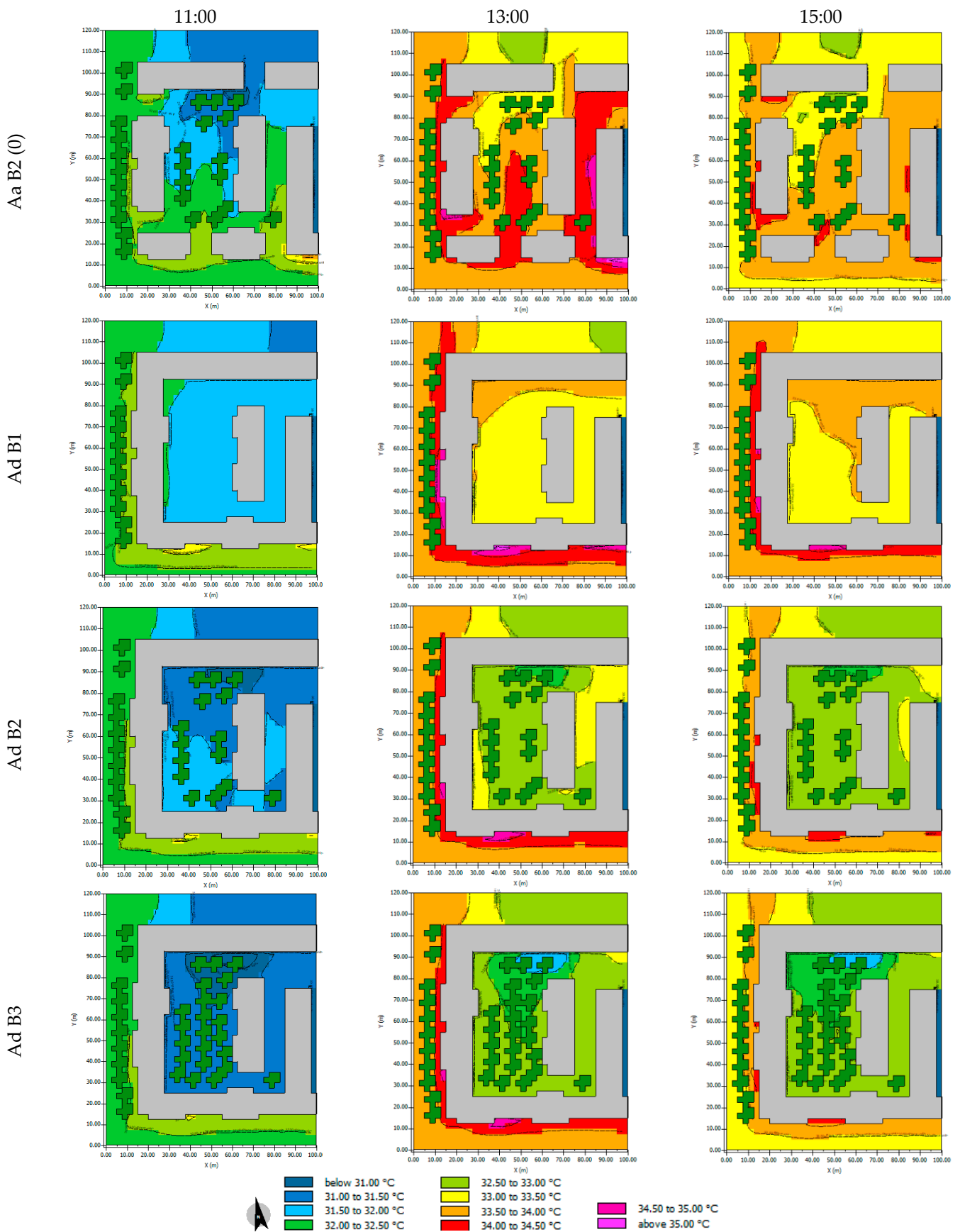
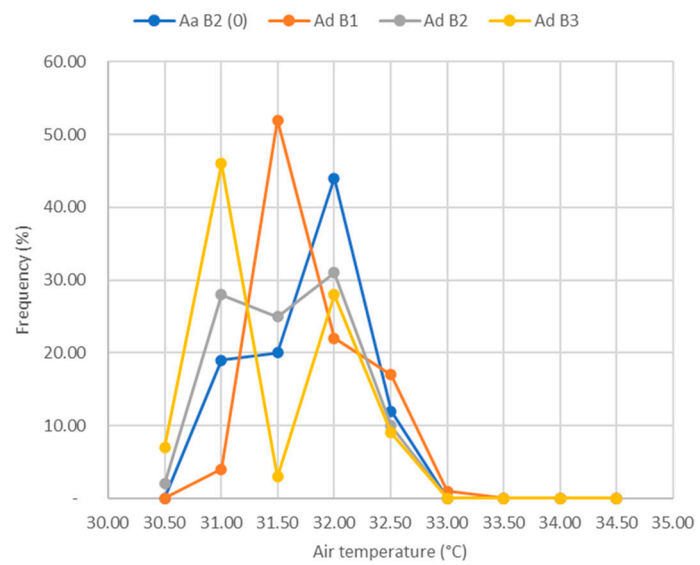
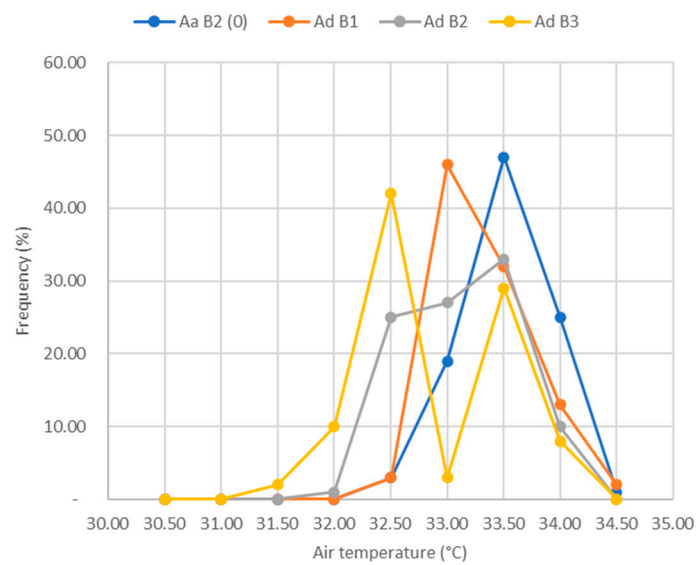


Figure 12. OMM showing the effects of variable (B) tree density effect—air temperature.

11:00



13:00



15:00

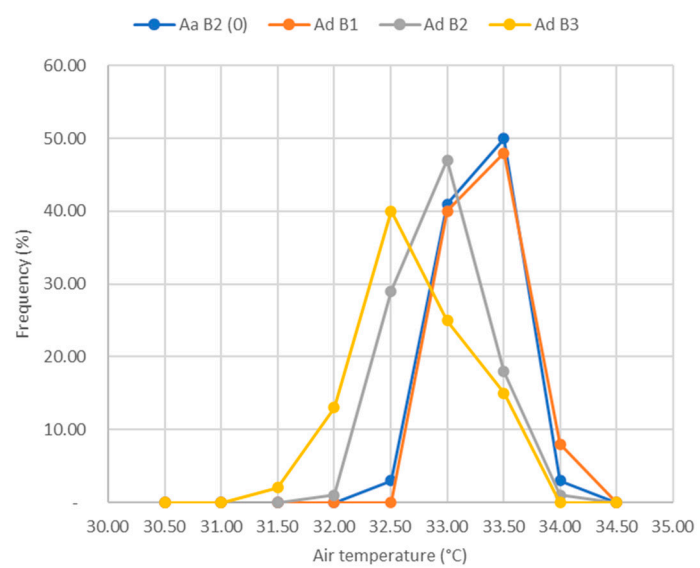


Figure 13. Variable B: OMM frequency of air temperature, per selected hours and scenarios.

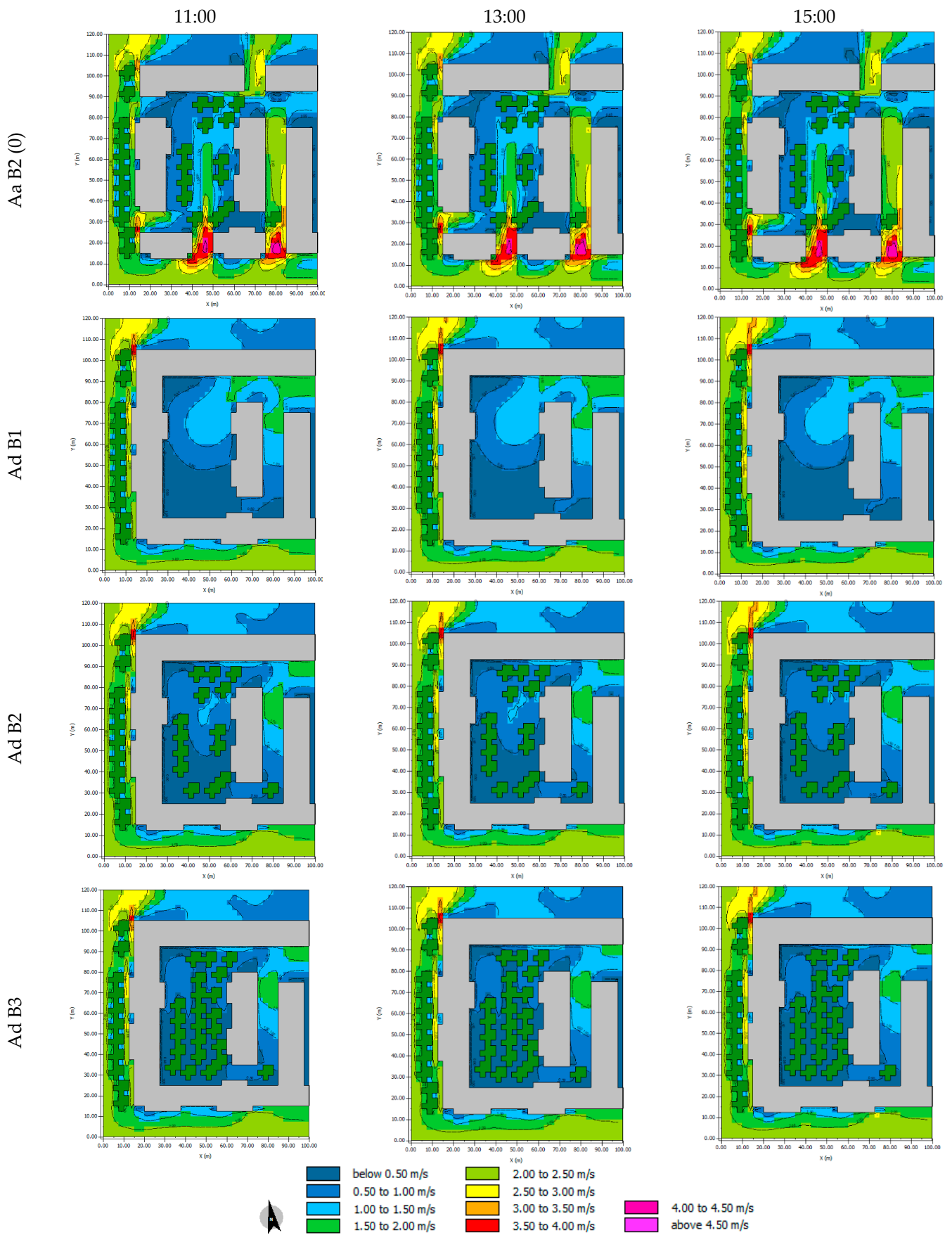
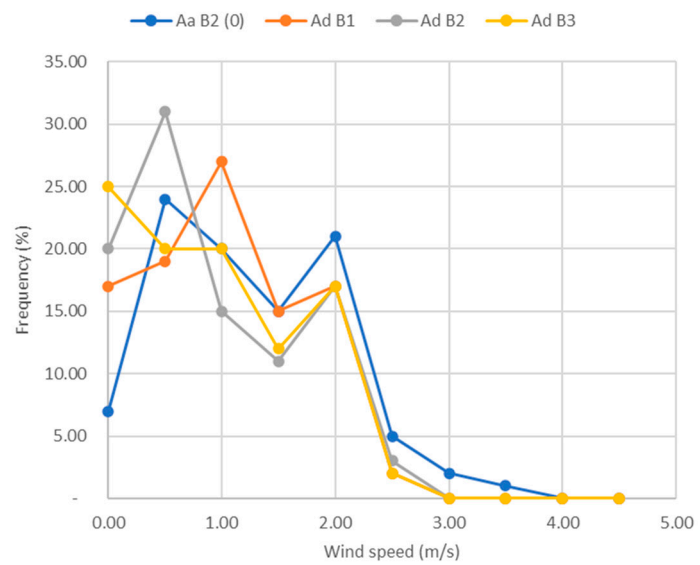
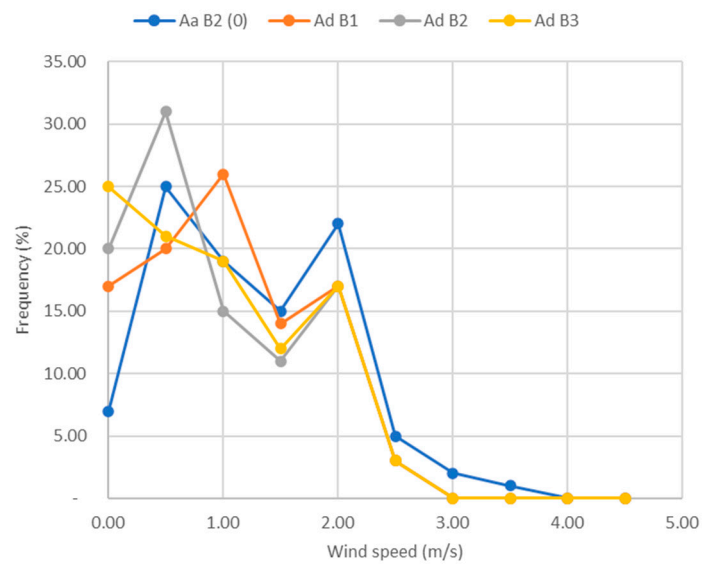


Figure 14. OMM showing the effects of variable (B) tree density effect—wind speed.

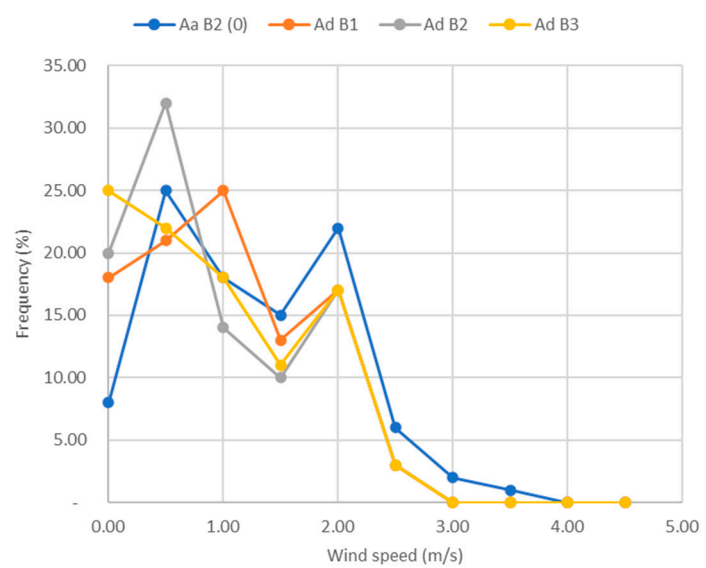
11:00



13:00



15:00

**Figure 15.** Variable B: OMM frequency of wind speed, per selected hours and scenarios.

The PET graphs (Figure 16) confirm the no-trees scenario as the most uncomfortable. In all three graphs, the highest frequency is found for ‘hot’ PET values (29 °C–35 °C, yellow). Again, it is interesting to evaluate the extreme situations, in particular the frequency of ‘extremely hot’ and ‘warm’ areas in the different scenarios. At 11:00, in the high-tree-density scenario (Ad B3), about 10% of the area is ‘warm’ (23 °C–29 °C), while in the no-trees scenario (Ad B1), this value is zero. At 13:00 and 15:00, the ‘warm’ area is absent for scenario Ad B3 too.

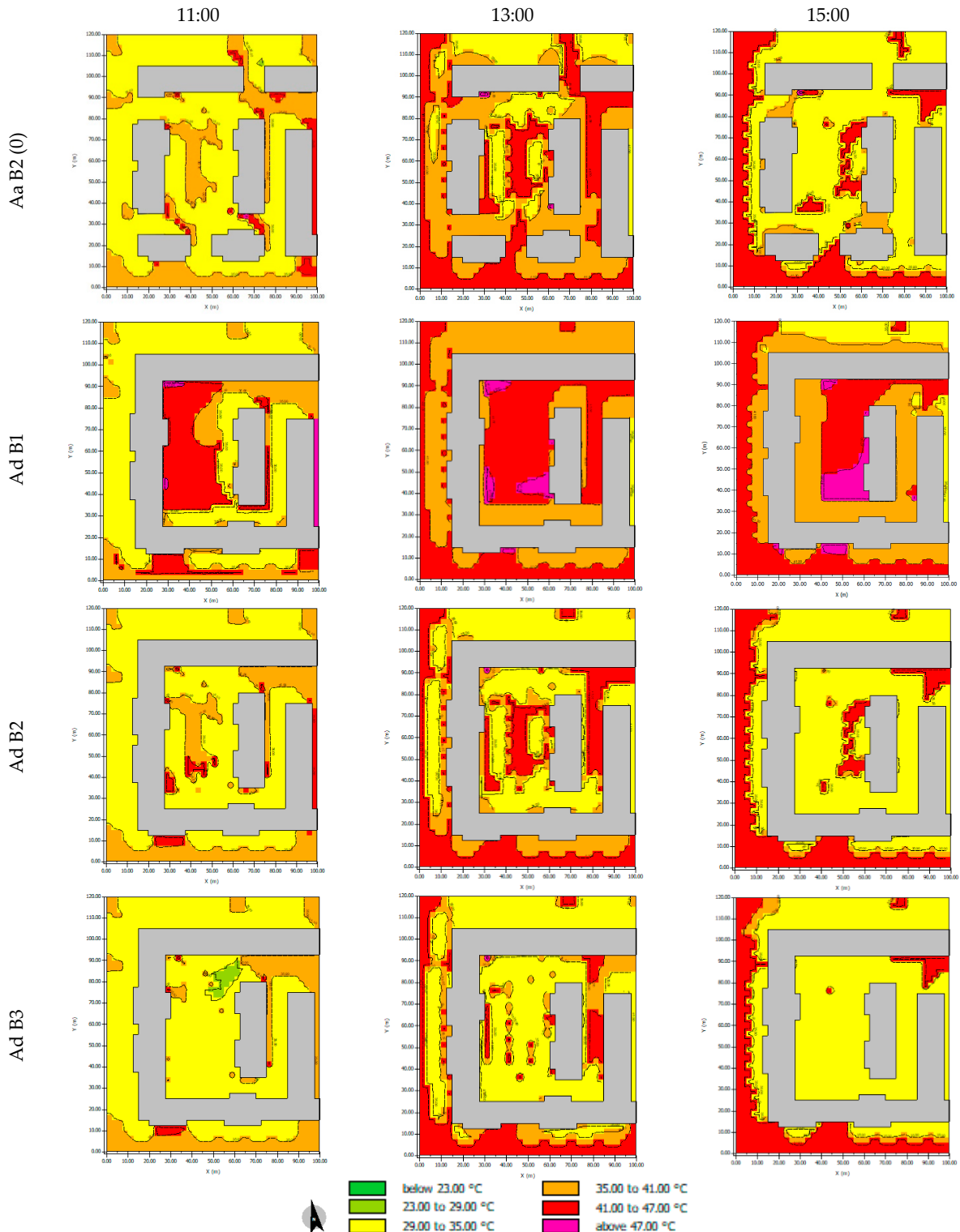
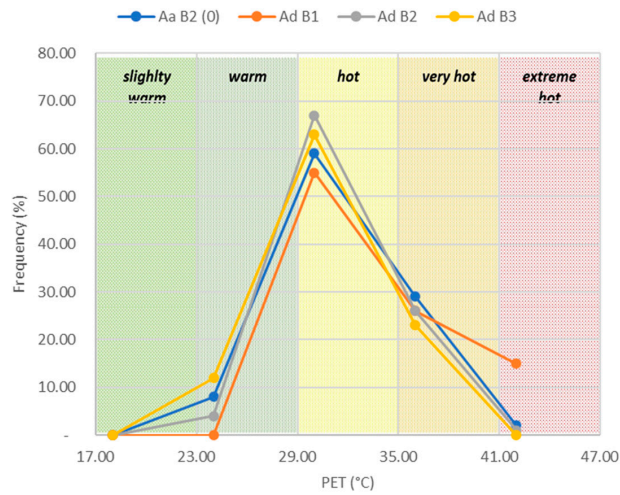


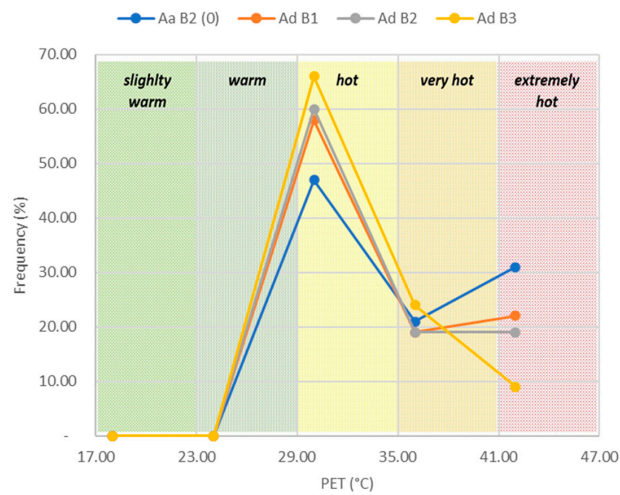
Figure 16. OMM showing the effects of variable (B) tree density effect—PET.

Figure 17 shows the frequency analysis. Looking at the values of the ‘extremely hot’ areas, in the no-trees scenario (Ad B1), the percentage of areas in the extreme condition is equal to 15% at 11:00, 25% at 13:00 and 20% at 15:00. On the contrary, in the scenario with high tree density (Ad B3), these percentages are 0%, 10%, and 8%, respectively, mostly due to the values outside the courtyard (borderline).

11:00



13:00



15:00

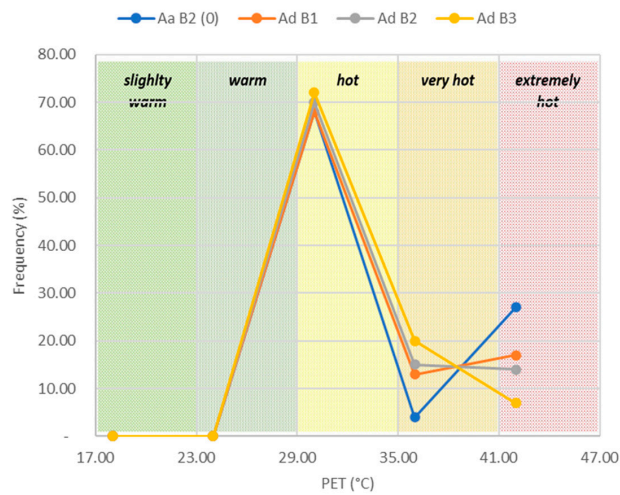


Figure 17. Variable B: OMM frequency of PET, per selected hours and scenarios.

5.3. Discussion

The in-depth investigation of frequency graphs and OMMs revealed some important reflections regarding the general impact of the two design variables examined in this study. The outcomes give some early insights on their effects and confirms the relevance of the issue that deserve further studies and applications to improve outdoor microclimate in courtyard buildings. First, it was proven that the courtyard microclimate and outdoor thermal comfort are significantly impacted by both the treatment and positioning of gaps. Changes in tree density also have a relevance. The gaps along the courtyard border may affect the projected shading on the courtyard, and thus the amount of solar radiation directly impacting the pavement, and partially also that reflected by buildings themselves. As a result, air temperature values change: the greater the shaded surface inside the courtyard, the lower the air temperature.

Regarding wind speed, instead, the presence or not of gaps does not impact significantly. Instead, the presence or absence of gaps has little impact on wind speed. Due to the Venturi effect, small variations may arise close to gaps with little improvement in comfort from increased airflow. Unfortunately, this can generate the movement of dust and particulates, causing other discomfort. For more accurate results, this limited effect of gap configuration on wind speed could be further investigated by means of CFD software, which is envisaged in a further stage of the study.

Breach positioning and treatment on the building perimeter do not significantly affect PET values, which are mainly dependent on projected building shadow. However, small variations are detected in mere gaps, with higher PET values, which is likely due to the higher solar radiation on the floor.

Vegetation results in great effects on air temperature and even more so on PET. For the proposed case study, the authors have intentionally decided to simulate vegetation combined with the 'all possible gaps filled' scenario, in order to exclude the contribution of the Venturi effect or solar radiation near gaps. As foreseeable, results for the no-trees scenario are all worsening the actual situation, especially regarding PET. Generally speaking, the other scenarios demonstrate that tree planting can improve the comfort level, decreasing heat stress even by two classes. The analysis of the graphs confirms that—thanks to the shade of the foliage and evapotranspiration—trees allow for greater comfort in the courtyard area. The comparison of the average/high-tree-density scenarios shows some differences, but does not suggest a visible preference to define a minimum tree density threshold, which definitely should be tuned according to the local context.

Overall, the strength of the proposed procedure lies especially in the possibility to simulate the effects of diverse intervention scenarios and the related impact of possible replication within the same urban area. As a means of example, the Bolognina district, where the case study is located (Figure 3), has over 15 courtyard buildings similar in characteristics and size to the simulated one. Considering air temperature, which is the parameter most affected by changes in the comfort variables, from Table 1 it can be observed that at 11:00 a.m. in simulation B3, most of the area is at 31 °C, while in scenarios 0 and B2, the air temperature is 32 °C, and 31.5 °C in B1. At 13:00, the difference between the four scenarios is comparable, but with temperature values about 1.5 °C higher. At 15:00 in scenarios 0 and B1, most of the courtyard is at 33.5 °C, while scenario B3 is at 32.5 °C. In other words, scenario B3 registers a reduction of at least 1 °C in air temperature during the hottest hours of the day.

Table 1. Frequency of air temperature distribution according to variable B. Highlighted values are those most relevant to the discussion.

Hours	Air Temperature (°C)	Aa B2 (0)	Ad B1	Ad B2	Ad B3
11:00	30.50	-	-	2.00	7.00
	31.00	19.00	4.00	28.00	46.00
	31.50	20.00	52.00	25.00	3.00
	32.00	44.00	22.00	31.00	28.00
	32.50	12.00	17.00	10.00	9.00
	33.00	-	1.00	-	-
	33.50	-	-	-	-
	34.00	-	-	-	-
	34.50	-	-	-	-
	13:00	30.50	-	-	-
31.00		-	-	-	-
31.50		-	-	-	2.00
32.00		-	-	1.00	10.00
32.50		3.00	3.00	25.00	42.00
33.00		19.00	46.00	27.00	3.00
33.50		47.00	32.00	33.00	29.00
34.00		25.00	13.00	10.00	8.00
34.50		1.00	2.00	-	-
15:00		30.50	-	-	-
	31.00	-	-	-	-
	31.50	-	-	-	2.00
	32.00	-	-	1.00	13.00
	32.50	3.00	-	29.00	40.00
	33.00	41.00	40.00	47.00	25.00
	33.50	50.00	48.00	18.00	15.00
	34.00	3.00	8.00	1.00	-
	34.50	-	-	-	-

Accordingly, if the 2100 m² of the case study courtyard is assumed as a base unit for the whole courts of the 15 similar plots (although others of a different size could also be potentially involved), a surface of approximately 3.15 hectares would be potentially mitigated, reducing the average temperature by 1 °C, with significant benefit for the whole residential area and the local community.

The explored replicability potential only refers to air temperature when varying tree density (B), as they have been proven to be the main difference generator in terms of mitigative impact. As mentioned, the continuity or the interruption of the courtyard's building fronts does not influence the overall conditions so remarkably as to justify their recurrent application, due to the possible limitations given by the urban fabric layout and to the related costs. Further studies in this field might be performed to increase the number of scenarios, or even variables to be combined. For the presented case study, a number of relevant scenarios have been selected to demonstrate the relevance of the topic, but authors are aware that many others could have been chosen and explored.

The procedure led to some general insights that are valid for the local climate (Bologna), and not necessarily for others. As such, it could be interesting to evaluate differences in the impact of the selected variables for diverse climatic zones or urban typologies, expanding the reflection to other contexts.

6. Conclusions

Large public areas, squares, public and private buildings (e.g., green roofs and reflective materials), as well as private open spaces, like courtyards, can all be targets of interventions to mitigate heat island effects in cities. That is why outdoor thermal comfort and mitigation strategies have been largely studied in recent decades, but still significant gaps are detected, and further research is needed to support the effective implementation of such actions into a more comprehensive framework that particularly considers the intermediate scale between the building and the district level.

Focusing on courtyard buildings, the case study's findings demonstrate the impact of vegetation in lowering air temperature and enhancing outdoor comfort (PET), while the presence or not of gaps along the courtyard borders appear less relevant and more difficult to replicate for other constraints that might depend on the urban fabric layout.

On this basis, the study provides a starting point for a research methodology that aims to identify patterns in the reconfiguration of private areas. In other words, the approach and the outcomes are applicable to a single courtyard and can be repeated to provide the same advantage in other private courtyards throughout the city. In this regard, it is important to highlight the distinction between the advantages of PET and the reduction in air temperature when discussing the benefits of the interventions. If repeated in several cases, the drop in air temperature helps lessen the effects of heat islands and heat waves, though neither of these phenomena can be eliminated because they rely on several variables, including the previously mentioned public areas and building exteriors.

Nevertheless, even small improvements in PET values allow for the achievement of another type of benefit related to the liveability of open spaces, which is the possibility to use the cooler ones (PET values below 35 °C) during hot summer days.

The described methodology has high replicability potential, as it proposes to investigate variations in OMM by ENVI-met and frequency graphs through a general concept that can be implemented in several other case studies (Figure 1). The idea behind it is that all the courtyard building-based urban patterns can be analysed through the proposed methodology in all urban patterns (such as Bologna or Barcelona) where this building typology is recurrent. The proposed demonstration case is therefore used to showcase the process and its outcome potential while discussing the methodological structure.

Software such as ENVI-met allows the simulation of diverse scenarios within the digital environment, and it is common knowledge that these increase their accuracy and relevance as the model scale enlarges (e.g., up to large city areas). Therefore, even if this study has focused on courtyard buildings, the same procedure can be extended to entire urban areas, including other open space typologies such as squares, streets, parks, etc.

The potential of the study lays in the presented methodology to combine several design variables, including, among the others, one of the most implemented NBSs to improve urban microclimate, that is, tree planting. This represents indeed a novel perspective to evaluate their benefits, which are usually discussed in terms of biophilia and shading contribution [82–84], and not for the overall benefits brought to outdoor thermal comfort.

Author Contributions: Conceptualisation, K.F., L.M. and J.G.; methodology, K.F., L.M. and J.G.; formal analysis, K.F. and L.M.; investigation, K.F. and L.M.; resources, K.F., L.M. and J.G.; data curation, K.F. and L.M.; writing—original draft preparation, L.M. and K.F.; writing—review and editing, K.F., L.M. and J.G.; supervision, J.G. All authors have read and agreed to the published version of the manuscript.

Funding: This research received no external funding.

Data Availability Statement: Data sharing not applicable.

Acknowledgments: The authors thank Isli Beijtaga for contributing to the data collection and ENVI-met simulation stages.

Conflicts of Interest: The authors declare no conflict of interest.

References

1. IPCC. *Climate Change 2022: Mitigation of Climate Change—Contribution of Working Group III to the Sixth Assessment Report of the Intergovernmental Panel on Climate Change*; Shukla, P.R., Skea, J., Slade, R., Al Khourdajie, A., van Diemen, R., McCollum, D., Pathak, M., Some, S., Vyas, P., Fradera, R., et al., Eds.; Cambridge University Press: Cambridge, UK; New York, NY, USA, 2022.
2. Spano, D.; Armiento, M.; Aslam, M.F.; Bacciu, V.; Bigano, A.; Bosello, F.; Breil, M.; Buonocore, M.; Butenschön, M.; Cadau, M.; et al. *G20 Climate Risk Atlas: Impacts, Policy, Economics*; European Union: Brussels, Belgium, 2021.
3. Oke, T.R. City Size and the Urban Heat Island. *Atmos. Environ.* **1973**, *7*, 769–779. [[CrossRef](#)]
4. IPCC Working Group I. *IPCC Fourth Assessment Report: Climate Change 2007*; IPCC: Geneva, Switzerland, 2007.
5. Ma, X.; Peng, S. Assessing the Quantitative Relationships between the Impervious Surface Area and Surface Heat Island Effect during Urban Expansion. *PeerJ* **2021**, *9*, e11854. [[CrossRef](#)]
6. Almeida, C.R.d.; Teodoro, A.C.; Gonçalves, A. Study of the Urban Heat Island (UHI) Using Remote Sensing Data/Techniques: A Systematic Review. *Environments* **2021**, *8*, 105. [[CrossRef](#)]
7. Hsieh, C.-M.; Huang, H.-C. Mitigating Urban Heat Islands: A Method to Identify Potential Wind Corridor for Cooling and Ventilation. *Comput. Environ. Urban Syst.* **2016**, *57*, 130–143. [[CrossRef](#)]
8. Krüger, E.L.; Minella, F.O.; Rasia, F. Impact of Urban Geometry on Outdoor Thermal Comfort and Air Quality from Field Measurements in Curitiba, Brazil. *Build. Environ.* **2011**, *46*, 621–634. [[CrossRef](#)]
9. Gál, T.; Sümeghy, Z. Mapping the Roughness Parameters in Large Urban Area for Urban Climate Applications. *Acta Climatol. Chronol.* **2007**, *27*–36.
10. Emmanuel, R. *An Urban Approach to Climate Sensitive Design: Strategies for the Tropics*; Taylor & Francis: Abingdon, UK, 2012.
11. Mohammad Harmay, N.S.; Choi, M. The Urban Heat Island and Thermal Heat Stress Correlate with Climate Dynamics and Energy Budget Variations in Multiple Urban Environments. *Sustain. Cities Soc.* **2023**, *91*, 104422. [[CrossRef](#)]
12. Na, W.; Jang, J.-Y.; Lee, K.E.; Kim, H.; Jun, B.; Kwon, J.-W.; Jo, S.-N. The Effects of Temperature on Heat-Related Illness According to the Characteristics of Patients during the Summer of 2012 in the Republic of Korea. *J. Prev. Med. Public Health* **2013**, *46*, 19–27. [[CrossRef](#)]
13. Nanayakkara, S.; Wang, W.; Cao, J.; Wang, J.; Zhou, W. Analysis of Urban Heat Island Effect, Heat Stress and Public Health in Colombo, Sri Lanka and Shenzhen, China. *Atmosphere* **2023**, *14*, 839. [[CrossRef](#)]
14. Elnabawi, M.H.; Hamza, N. Outdoor Thermal Comfort: Coupling Microclimatic Parameters with Subjective Thermal Assessment to Design Urban Performative Spaces. *Buildings* **2020**, *10*, 238. [[CrossRef](#)]
15. Copernicus. Demonstrating Heat Stress in European Cities. Available online: <https://climate.copernicus.eu/demonstrating-heat-stress-european-cities> (accessed on 5 June 2023).
16. Fadhil, M.; Hamoodi, M.N.; Ziboon, A.R.T. Mitigating Urban Heat Island Effects in Urban Environments: Strategies and Tools. *IOP Conf. Ser. Earth Environ. Sci.* **2023**, *1129*, 012025. [[CrossRef](#)]
17. C40 Cities Climate Leadership Group. How to Adapt Your City to Extreme Heat. Available online: https://www.c40knowledgehub.org/s/article/How-to-adapt-your-city-to-extreme-heat?language=en_US (accessed on 14 March 2023).
18. Tsoka, S.; Tsikaloudaki, K.; Theodosiou, T.; Bikas, D. Urban Warming and Cities' Microclimates: Investigation Methods and Mitigation Strategies—A Review. *Energies* **2020**, *13*, 1414. [[CrossRef](#)]
19. Saneinejad, S.; Moonen, P.; Carmeliet, J. Comparative Assessment of Various Heat Island Mitigation Measures. *Build. Environ.* **2014**, *73*, 162–170. [[CrossRef](#)]
20. Zhang, S.; Li, S.; Shu, L.; Xiao, T.; Shui, T. Landscape Configuration Effects on Outdoor Thermal Comfort across Campus—A Case Study. *Atmosphere* **2023**, *14*, 270. [[CrossRef](#)]
21. Vujovic, S.; Haddad, B.; Karaky, H.; Sebaibi, N.; Boutouil, M. Urban Heat Island: Causes, Consequences, and Mitigation Measures with Emphasis on Reflective and Permeable Pavements. *CivilEng* **2021**, *2*, 459–484. [[CrossRef](#)]
22. Wardeh, Y.; Kinab, E.; Escadeillas, G.; Rahme, P.; Ginestet, S. Review of the Optimization Techniques for Cool Pavements Solutions to Mitigate Urban Heat Islands. *Build. Environ.* **2022**, *223*, 109482. [[CrossRef](#)]
23. Kappou, S.; Souliotis, M.; Papaefthimiou, S.; Panaras, G.; Paravantis, J.A.; Michalena, E.; Hills, J.M.; Vouros, A.P.; Ntymenou, A.; Mihalakakou, G. Cool Pavements: State of the Art and New Technologies. *Sustainability* **2022**, *14*, 5159. [[CrossRef](#)]
24. Fabbri, K.; Gaspari, J.; Costa, A.; Principi, S. The Role of Architectural Skin Emissivity Influencing Outdoor Microclimatic Comfort: A Case Study in Bologna, Italy. *Sustainability* **2022**, *14*, 14669. [[CrossRef](#)]
25. Alonso, C.; Martín-Consuegra, F.; Oteiza, I.; Asensio, E.; Pérez, G.; Martínez, I.; Frutos, B. Effect of Façade Surface Finish on Building Energy Rehabilitation. *Sol. Energy* **2017**, *146*, 470–483. [[CrossRef](#)]
26. Zinzi, M. Exploring the Potentialities of Cool Facades to Improve the Thermal Response of Mediterranean Residential Buildings. *Sol. Energy* **2016**, *135*, 386–397. [[CrossRef](#)]
27. Rosso, F.; Pisello, A.L.; Pignatta, G.; Castaldo, V.L.; Piselli, C.; Cotana, F.; Ferrero, M. Outdoor Thermal and Visual Perception of Natural Cool Materials for Roof and Urban Paving. *Procedia Eng.* **2015**, *118*, 1325–1332. [[CrossRef](#)]
28. Zeeshan, M.; Ali, Z. The Potential of Cool Materials towards Improving Thermal Comfort Conditions inside Real-Urban Hot-Humid Microclimate. *Environ. Urban. ASIA* **2022**, *13*, 56–72. [[CrossRef](#)]
29. Fabbri, K.; Gaspari, J.; Bartoletti, S.; Antonini, E. Effect of Façade Reflectance on Outdoor Microclimate: An Italian Case Study. *Sustain. Cities Soc.* **2020**, *54*, 101984. [[CrossRef](#)]

30. Gál, T.; Mahó, S.I.; Skarbit, N.; Unger, J. Numerical Modelling for Analysis of the Effect of Different Urban Green Spaces on Urban Heat Load Patterns in the Present and in the Future. *Comput. Environ. Urban Syst.* **2021**, *87*, 101600. [CrossRef]
31. EPA. Reduce Urban Heat Island Effect. Available online: <https://www.epa.gov/green-infrastructure/reduce-urban-heat-island-effect> (accessed on 10 May 2023).
32. Goldbach, A.; Kuttler, W. Influence of Evapotranspiration on Thermal Comfort in Central European Cities. In Proceedings of the EGU General Assembly 2012, Vienna, Austria, 22–27 April 2012; Volume 14, p. 5396.
33. Yang, L.; Yu, K.; Ai, J.; Liu, Y.; Lin, L.; Lin, L.; Liu, J. The Influence of Green Space Patterns on Land Surface Temperature in Different Seasons: A Case Study of Fuzhou City, China. *Remote Sens.* **2021**, *13*, 5114. [CrossRef]
34. Zhou, W.; Yu, W.; Zhang, Z.; Cao, W.; Wu, T. How Can Urban Green Spaces Be Planned to Mitigate Urban Heat Island Effect under Different Climatic Backgrounds? A Threshold-Based Perspective. *Sci. Total Environ.* **2023**, *890*, 164422. [CrossRef]
35. Gunawardena, K.R.; Wells, M.J.; Kershaw, T. Utilising Green and Bluespace to Mitigate Urban Heat Island Intensity. *Sci. Total Environ.* **2017**, *584–585*, 1040–1055. [CrossRef] [PubMed]
36. Li, Y.; Zhao, Z.; Xin, Y.; Xu, A.; Xie, S.; Yan, Y.; Wang, L. How Are Land-Use/Land-Cover Indices and Daytime and Nighttime Land Surface Temperatures Related in Eleven Urban Centres in Different Global Climatic Zones? *Land* **2022**, *11*, 1312. [CrossRef]
37. Seddon, N.; Chausson, A.; Berry, P.; Girardin, C.A.J.; Smith, A.; Turner, B. Understanding the Value and Limits of Nature-Based Solutions to Climate Change and Other Global Challenges. *Philos. Trans. R. Soc. B Biol. Sci.* **2020**, *375*, 20190120. [CrossRef]
38. Johansson, E. Influence of Urban Geometry on Outdoor Thermal Comfort in a Hot Dry Climate: A Study in Fez, Morocco. *Build. Environ.* **2006**, *41*, 1326–1338. [CrossRef]
39. Banerjee, S.; Ching, N.Y.G.; Yik, S.K.; Dzyuban, Y.; Crank, P.J.; Pek Xin Yi, R.; Chow, W.T.L. Analysing Impacts of Urban Morphological Variables and Density on Outdoor Microclimate for Tropical Cities: A Review and a Framework Proposal for Future Research Directions. *Build. Environ.* **2022**, *225*, 109646. [CrossRef]
40. Yang, C.; Zhu, W.; Sun, J.; Xu, X.; Wang, R.; Lu, Y.; Zhang, S.; Zhou, W. Assessing the Effects of 2D/3D Urban Morphology on the 3D Urban Thermal Environment by Using Multi-Source Remote Sensing Data and UAV Measurements: A Case Study of the Snow-Climate City of Changchun, China. *J. Clean. Prod.* **2021**, *321*, 128956. [CrossRef]
41. Li, Z.; Hu, D. Exploring the Relationship between the 2D/3D Architectural Morphology and Urban Land Surface Temperature Based on a Boosted Regression Tree: A Case Study of Beijing, China. *Sustain. Cities Soc.* **2022**, *78*, 103392. [CrossRef]
42. Gao, Y.; Zhao, J.; Han, L. Exploring the Spatial Heterogeneity of Urban Heat Island Effect and Its Relationship to Block Morphology with the Geographically Weighted Regression Model. *Sustain. Cities Soc.* **2022**, *76*, 103431. [CrossRef]
43. Palusci, O.; Monti, P.; Cecere, C.; Montazeri, H.; Blocken, B. Impact of Morphological Parameters on Urban Ventilation in Compact Cities: The Case of the Tuscolano-Don Bosco District in Rome. *Sci. Total Environ.* **2022**, *807*, 150490. [CrossRef]
44. Palusci, O.; Cecere, C. Urban Ventilation in the Compact City: A Critical Review and a Multidisciplinary Methodology for Improving Sustainability and Resilience in Urban Areas. *Sustainability* **2022**, *14*, 3948. [CrossRef]
45. Lin, M.; Hang, J.; Li, Y.; Luo, Z.; Sandberg, M. Quantitative Ventilation Assessments of Idealized Urban Canopy Layers with Various Urban Layouts and the Same Building Packing Density. *Build. Environ.* **2014**, *79*, 152–167. [CrossRef]
46. Oke, T.R. Street Design and Urban Canopy Layer Climate. *Energy Build.* **1988**, *11*, 103–113. [CrossRef]
47. Chandler, D.L. Urban Heat Island Effects Depend on a City’s Layout; MIT News Office. Available online: <https://news.mit.edu/2018/urban-heat-island-effects-depend-city-layout-0222> (accessed on 12 February 2023).
48. Taleghani, M.; Tenpierik, M.; van den Dobbelaer, A.; Sailor, D.J. Heat in Courtyards: A Validated and Calibrated Parametric Study of Heat Mitigation Strategies for Urban Courtyards in the Netherlands. *Sol. Energy* **2014**, *103*, 108–124. [CrossRef]
49. Ghaffarianhoseini, A.; Berardi, U.; Ghaffarianhoseini, A. Thermal Performance Characteristics of Unshaded Courtyards in Hot and Humid Climates. *Build. Environ.* **2015**, *87*, 154–168. [CrossRef]
50. Almhafdy, A.; Ibrahim, N.; Ahmad, S.S.; Yahya, J. Courtyard Design Variants and Microclimate Performance. *Procedia Soc. Behav. Sci.* **2013**, *101*, 170–180. [CrossRef]
51. Li, M.; Jin, Y.; Guo, J. Dynamic Characteristics and Adaptive Design Methods of Enclosed Courtyard: A Case Study of a Single-Story Courtyard Dwelling in China. *Build. Environ.* **2022**, *223*, 109445. [CrossRef]
52. Martinelli, L.; Matzarakis, A. Influence of Height/Width Proportions on the Thermal Comfort of Courtyard Typology for Italian Climate Zones. *Sustain. Cities Soc.* **2017**, *29*, 97–106. [CrossRef]
53. Han, J.; Li, X.; Li, B.; Yang, W.; Yin, W.; Peng, Y.; Feng, T. Research on the Influence of Courtyard Space Layout on Building Microclimate and Its Optimal Design. *Energy Build.* **2023**, *289*, 113035. [CrossRef]
54. Garcia-Nevado, E.; Beckers, B.; Coch, H. Assessing the Cooling Effect of Urban Textile Shading Devices Through Time-Lapse Thermography. *Sustain. Cities Soc.* **2020**, *63*, 102458. [CrossRef]
55. Cantini, A.; Angelotti, A.; Zanelli, A. A lightweight textile device for urban microclimate control and thermal comfort improvement: Concept project and design parameters. In *Softening the Habitats—Sustainable Innovation in Minimal Mass Structures and Lightweight Architectures*; Maggioli Editore: Santarcangelo di Romagna, Italy, 2019. [CrossRef]
56. López-Cabeza, V.P.; Galán-Marín, C.; Rivera-Gómez, C.; Roa-Fernández, J. Courtyard Microclimate ENVI-Met Outputs Deviation from the Experimental Data. *Build. Environ.* **2018**, *144*, 129–141. [CrossRef]
57. Wu, R.; Fang, X.; Liu, S.; Middel, A. A Fast and Accurate Mean Radiant Temperature Model for Courtyards: Evidence from the Keyuan Garden in Central Guangdong, China. *Build. Environ.* **2023**, *229*, 109916. [CrossRef]

58. Höpfe, P. The Physiological Equivalent Temperature—A Universal Index for the Biometeorological Assessment of the Thermal Environment. *Int. J. Biometeorol.* **1999**, *43*, 71–75. [CrossRef]
59. Safarzadeh, H.; Bahadori, M.N. Passive Cooling Effects of Courtyards. *Build. Environ.* **2005**, *40*, 89–104. [CrossRef]
60. Soflaei, F.; Shokouhian, M.; Abraveshdar, H.; Alipour, A. The Impact of Courtyard Design Variants on Shading Performance in Hot- Arid Climates of Iran. *Energy Build.* **2017**, *143*, 71–83. [CrossRef]
61. Forouzandeh, A. Numerical Modeling Validation for the Microclimate Thermal Condition of Semi-Closed Courtyard Spaces between Buildings. *Sustain. Cities Soc.* **2018**, *36*, 327–345. [CrossRef]
62. Li, J.; Zheng, B.; Bedra, K.B. Evaluating the Improvements of Thermal Comfort by Different Natural Elements within Courtyards in Singapore. *Urban Clim.* **2022**, *45*, 101253. [CrossRef]
63. Taleghani, M.; Tenpierik, M.; van den Dobbelen, A. Indoor Thermal Comfort in Urban Courtyard Block Dwellings in the Netherlands. *Build. Environ.* **2014**, *82*, 566–579. [CrossRef]
64. Li, J.; Liu, J.; Srebric, J.; Hu, Y.; Liu, M.; Su, L.; Wang, S. The Effect of Tree-Planting Patterns on the Microclimate within a Courtyard. *Sustainability* **2019**, *11*, 1665. [CrossRef]
65. Zhao, Y.; Chen, Y.; Li, K. A Simulation Study on the Effects of Tree Height Variations on the Façade Temperature of Enclosed Courtyard in North China. *Build. Environ.* **2022**, *207*, 108566. [CrossRef]
66. Ngo, H.N.D.; Motoasca, E.; Versele, A.; Pham, H.C.; Breesch, H. Effect of Neighbourhood Courtyard Design on the Outdoor Thermal Comfort in a Tropical City. *IOP Conf. Ser. Earth Environ. Sci.* **2022**, *1078*, 012035. [CrossRef]
67. Ferrari, S. Ventilation in a Group of Courtyard Buildings. *EPJ Web Conf.* **2022**, *264*, 01014. [CrossRef]
68. Aryani, S.M.; Sasongko, S.; Sulistyono, I.B.; Hidayati, N. Courtyard Placement for Maintaining Air Movement of Natural Ventilation inside a Transformed House. In Proceedings of the 4th Bandung Creative Movement International Conference on Creative Industries 2017 (BCM 2017), Bandung, Indonesia, 9–10 October 2017; Atlantis Press: Zhengzhou, China, 2018; pp. 355–359.
69. Sun, H.; Jimenez-Bescos, C.; Mohammadi, M.; Zhong, F.; Calautit, J.K. Numerical Investigation of the Influence of Vegetation on the Aero-Thermal Performance of Buildings with Courtyards in Hot Climates. *Energies* **2021**, *14*, 5388. [CrossRef]
70. Subhashini, S.; Thirumaran, K. CFD Simulations for Examining Natural Ventilation in the Learning Spaces of an Educational Building with Courtyards in Madurai. *Build. Serv. Eng. Res. Technol.* **2020**, *41*, 466–479. [CrossRef]
71. Maryland Department of Planning. Models and Guidelines for Infill Development. 2001. Available online: <https://planning.maryland.gov/Documents/OurProducts/Archive/72195/mg23-Infill-Development.pdf> (accessed on 12 February 2023).
72. MRSC. Infill Development. Available online: <https://mrsc.org/explore-topics/planning/development-types-and-land-uses/infill-development> (accessed on 10 June 2023).
73. Ottawa Council. Urban Design Guidelines for Low-Rise Infill Housing. 2022. Available online: <https://ottawa.ca/en/planning-development-and-construction/community-design/design-and-planning-guidelines/completed-guidelines/urban-design-guidelines-low-rise-infill-housing> (accessed on 12 February 2023).
74. Cardiff Council. Infill Sites Supplementary Planning Guidance. 2011. Available online: <https://www.cardiff.gov.uk/ENG/resident/Planning/Planning-Policy/Supplementary-Planning-Guidance/Documents/Infill%20Sites%20SPG%20-%20Nov%202017%20Final.pdf> (accessed on 11 February 2023).
75. Altunkasa, C.; Uslu, C. Use of Outdoor Microclimate Simulation Maps for a Planting Design to Improve Thermal Comfort. *Sustain. Cities Soc.* **2020**, *57*, 102137. [CrossRef]
76. Gaspari, J.; Fabbri, K. A Study on the Use of Outdoor Microclimate Map to Address Design Solutions for Urban Regeneration. *Energy Procedia* **2017**, *111*, 500–509. [CrossRef]
77. Fabbri, K.; Costanzo, V. Drone-Assisted Infrared Thermography for Calibration of Outdoor Microclimate Simulation Models. *Sustain. Cities Soc.* **2020**, *52*, 101855. [CrossRef]
78. Matzarakis, A.; Mayer, H.; Iziomon, M.G. Applications of a Universal Thermal Index: Physiological Equivalent Temperature. *Int. J. Biometeorol.* **1999**, *43*, 76–84. [CrossRef] [PubMed]
79. Kottek, M.; Grieser, J.; Beck, C.; Rudolf, B.; Rubel, F. World Map of the Köppen- Geiger Climate Classification Updated. *Meteorol. Z.* **2006**, *15*, 259–263. [CrossRef]
80. Dext3r Database. Available online: <https://simc.arpae.it/dext3r/> (accessed on 16 March 2023).
81. ARPAER. Weather Data Emilia-Romagna Region. Available online: www.arpae.it (accessed on 5 April 2022).
82. Wild, T.; Freitas, T.; Vandewoestijne, S.; Bulkeley, H.; Naumann, S.; Vojinović, Z.; Calfapietra, C.; Whiteoak, K.; European Commission—Directorate-General for Research and Innovation. *Nature-Based Solutions: State of the Art in EU-Funded Projects*; European Union: Luxembourg, 2020; ISBN 9789276173342.
83. Mahmoud, I.; Eugenio Morello, E. *Catalogue of Nature-Based Solution for Urban Regeneration Energy & Urban Planning Workshop—Final Report*; School of Architecture Urban Planning and Construction Engineering: Milano, Italy, 2019.
84. Dumitru, A.; European Commission. Directorate-General for Research and Innovation. *Evaluating the Impact of Nature-Based Solutions: A Handbook for Practitioners*; Publications Office of the European Union: Luxembourg, 2021; ISBN 9789276228219.

Disclaimer/Publisher’s Note: The statements, opinions and data contained in all publications are solely those of the individual author(s) and contributor(s) and not of MDPI and/or the editor(s). MDPI and/or the editor(s) disclaim responsibility for any injury to people or property resulting from any ideas, methods, instructions or products referred to in the content.